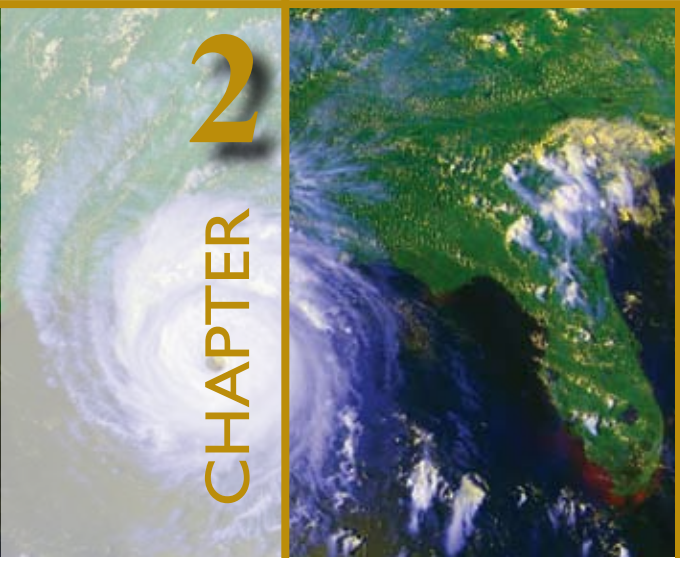

CHAPTER 2

# Observed Changes in Weather and Climate Extremes

***Convening Lead Author:*** Kenneth Kunkel, Univ. Ill. Urbana-Champaign, Ill. State Water Survey

***Lead Authors:*** Peter Bromirski, Scripps Inst. Oceanography, UCSD; Harold Brooks, NOAA; Tereza Cavazos, Centro de Investigación Científica y de Educación Superior de Ensenada, Mexico; Arthur Douglas, Creighton Univ.; David Easterling, NOAA; Kerry Emanuel, Mass. Inst. Tech.; Pavel Groisman, UCAR/NCDC; Greg Holland, NCAR; Thomas Knutson, NOAA; James Kossin, Univ. Wis., Madison, CIMSS; Paul Komar, Oreg. State Univ.; David Levinson, NOAA; Richard Smith, Univ. N.C., Chapel Hill

***Contributing Authors:*** Jonathan Allan, Oreg. Dept. Geology and Mineral Industries; Raymond Assel, NOAA; Stanley Changnon, Univ. Ill. Urbana-Champaign, Ill. State Water Survey; Jay Lawrimore, NOAA; Kam-biu Liu, La. State Univ., Baton Rouge; Thomas Peterson, NOAA

## KEY FINDINGS

### Observed Changes

Long-term upward trends in the frequency of unusually warm nights, extreme precipitation episodes, and the length of the frost-free season, along with pronounced recent increases in the frequency of North Atlantic tropical cyclones (hurricanes), the length of the frost-free season, and extreme wave heights along the West Coast are notable changes in the North American climate record.

- Most of North America is experiencing more unusually hot days. The number of warm spells has been increasing since 1950. However, the heat waves of the 1930s remain the most severe in the United States historical record back to 1895.
- There are fewer unusually cold days during the last few decades. The last 10 years have seen a lower number of severe cold waves than for any other 10-year period in the historical record which dates back to 1895. There has been a decrease in the number of frost days and a lengthening of the frost-free season, particularly in the western part of North America.
- Extreme precipitation episodes (heavy downpours) have become more frequent and more intense in recent decades than at any other time in the historical record, and account for a larger percentage of total precipitation. The most significant changes have occurred in most of the United States, northern Mexico, southeastern, northern and western Canada, and southern Alaska.
- There are recent regional tendencies toward more severe droughts in the southwestern United States, parts of Canada and Alaska, and Mexico.
- For much of the continental U.S. and southern Canada, the most severe droughts in the instrumental record occurred in the 1930s. While it is more meaningful to consider drought at the regional scale, there is no indication of an overall trend at the continental scale since 1895. In Mexico, the 1950s and 1994-present were the driest periods.
- Atlantic tropical cyclone (hurricane) activity, as measured by both frequency and the Power Dissipation Index (which combines storm

intensity, duration, and frequency) has increased. The increases are substantial since about 1970, and are likely substantial since the 1950s and 60s, in association with warming Atlantic sea surface temperatures. There is less confidence in data prior to about 1950.

- There have been fluctuations in the number of tropical storms and hurricanes from decade to decade, and data uncertainty is larger in the early part of the record compared to the satellite era beginning in 1965. Even taking these factors into account, it is likely that the annual numbers of tropical storms, hurricanes, and major hurricanes in the North Atlantic have increased over the past 100 years, a time in which Atlantic sea surface temperatures also increased.
- The evidence is less compelling for significant trends beginning in the late 1800s. The existing data for hurricane counts and one adjusted record of tropical storm counts both indicate no significant linear trends beginning from the mid- to late 1800s through 2005. In general, there is increasing uncertainty in the data as one proceeds back in time.
- There is no evidence for a long-term increase in North American mainland land-falling hurricanes.
- The hurricane Power Dissipation Index shows some increasing tendency in the western north Pacific since 1980. It has decreased since 1980 in the eastern Pacific, affecting the Mexican west coast and shipping lanes, but rainfall from near-coastal hurricanes has increased since 1949.

- The balance of evidence suggests that there has been a northward shift in the tracks of strong low pressure systems (storms) in both the North Atlantic and North Pacific basins. There is a trend toward stronger intense low pressure systems in the North Pacific.
- Increases in extreme wave height characteristics have been observed along the Pacific coast of North America during recent decades based on three decades of buoy data. These increases have been greatest in the Pacific Northwest, and are likely a reflection of changes in storm tracks.
- There is evidence for an increase in extreme wave height characteristics in the Atlantic since the 1970s, associated with more frequent and more intense hurricanes.
- Over the 20th century, there was considerable decade-to-decade variability in the frequency of snowstorms of six inches or more. Regional analyses suggest that there has been a decrease in snowstorms in the South and lower Midwest of the United States, and an increase in snowstorms in the upper Midwest and Northeast. This represents a northward shift in snowstorm occurrence, and this shift, combined with higher temperatures, is consistent with a decrease in snow cover extent over the United States. In northern Canada, there has also been an observed increase in heavy snow events (top 10% of storms) over the same time period. Changes in heavy snow events in southern Canada are dominated by decade-to-decade variability.

- There is no indication of continental scale trends in episodes of freezing rain during the 20th century.
- The data used to examine changes in the frequency and severity oftornadoes and severe thunderstorms are inadequate to make definitive statements about actual changes.
- The pattern of changes of ice storms varies by region.

## 2.1 BACKGROUND

Weather and climate extremes exhibit substantial spatial variability. It is not unusual for severe drought and flooding to occur simultaneously in different parts of North America (*e.g.*, catastrophic flooding in the Mississippi River basin and severe drought in the southeast United States during summer 1993). These reflect temporary shifts in large-scale circulation patterns that are an integral part of the climate system. The central goal of this chapter is to identify long-term shifts/trends in extremes and to characterize the continental-scale patterns of such shifts. Such characterization requires data sets that are homogeneous, of adequate length, and with continental-scale coverage. Many data sets meet these requirements for limited periods only. For temperature and precipitation, rather high quality data are available for the conterminous United States back to the late 19th century. However, shorter data records are available for parts of Canada, Alaska, Hawaii, Mexico, the Caribbean, and U.S. territories. In practice, this limits true continental-scale analyses of temperature and precipitation extremes to the middle part of the 20th century onward. Other phenomena have similar limitations, and continental-scale characterizations are generally limited to the last 50 to 60 years or less, or must confront data homogeneity issues which add uncertainty to the analysis. We consider all studies that are available, but in many cases these studies have to be interpreted carefully because of these limitations. A variety of statistical techniques are used in the studies cited here. General information about statistical methods along with several illustrative examples are given in Appendix A.

## 2.2 OBSERVED CHANGES AND VARIATIONS IN WEATHER AND CLIMATE EXTREMES

### 2.2.1 Temperature Extremes

Extreme temperatures do not always correlate with average temperature, but they often change in tandem; thus, average temperature changes provide a context for discussion of extremes. In 2005, virtually all of North America was above to much-above average[1] (Shein, 2006) and 2006 was the second hottest year on record in the conterminous United States (Arguez, 2007). The areas experiencing the largest temperature anomalies included the higher latitudes of Canada and Alaska. Annual average temperature time series for Canada, Mexico and the United States all show substantial warming since the middle of the 20th century (Shein, 2006). Since the record hot year of 1998, six of the past ten years (1998-2007) have had annual average temperatures that fall in the hottest 10% of all years on record for the U.S. Urban warming is a potential concern when considering temperature trends. However, recent work (*e.g.,* Peterson *et al.*, 2003; Easterling *et al.*, 1997) show that urban warming is only a small part of the observed warming since the late 1800s.

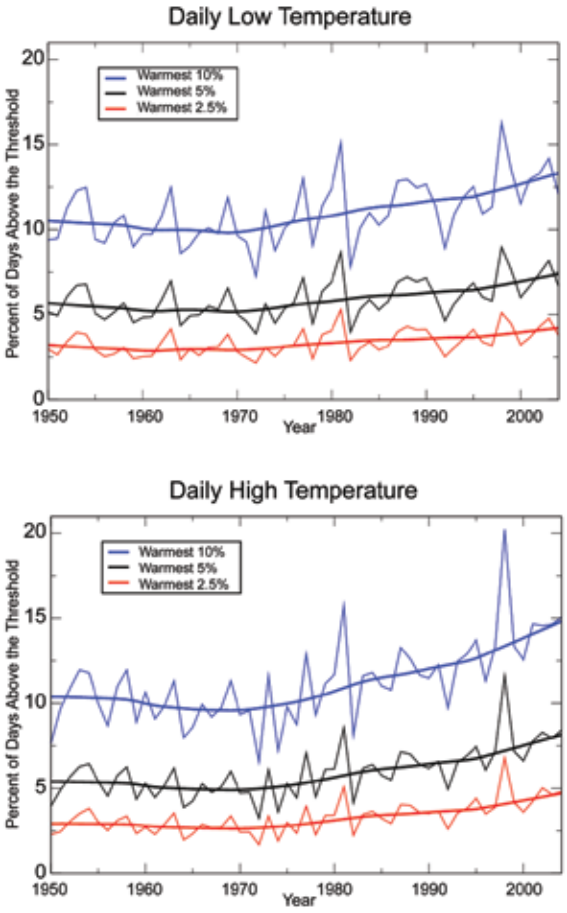


**Figure 2.1** Changes in the percentage of days in a year above three thresholds for North America for daily high temperature (top) and daily low temperature (bottom) (Peterson *et al.*, 2008).

Since 1950, the annual percent of days exceeding the 90th, 95th, and 97.5 percentile thresholds[2] for both maximum (hottest daytime highs) and minimum (warmest nighttime lows) temperature have increased when averaged over all of North America (Figure 2.1; Peterson *et al.,* 2008). The changes are greatest in the 90th percentile, increasing from about 10% of the

Annual average temperature time series for Canada, Mexico, and the United States all show substantial warming since the middle of the 20th century.

[1] NOAA's National Climatic Data Center uses the following terminology for classifying its monthly/seasonal/annual U.S. temperature and precipitation rankings: "near-normal" is defined as within the middle third, "above/below normal" is within the top third/bottom third, and "much-above/much-below normal" is within the top-tenth/bottom tenth of all such periods on record.

[2] An advantage of the use of percentile, rather than absolute thresholds, is that they account for regional climate differences.

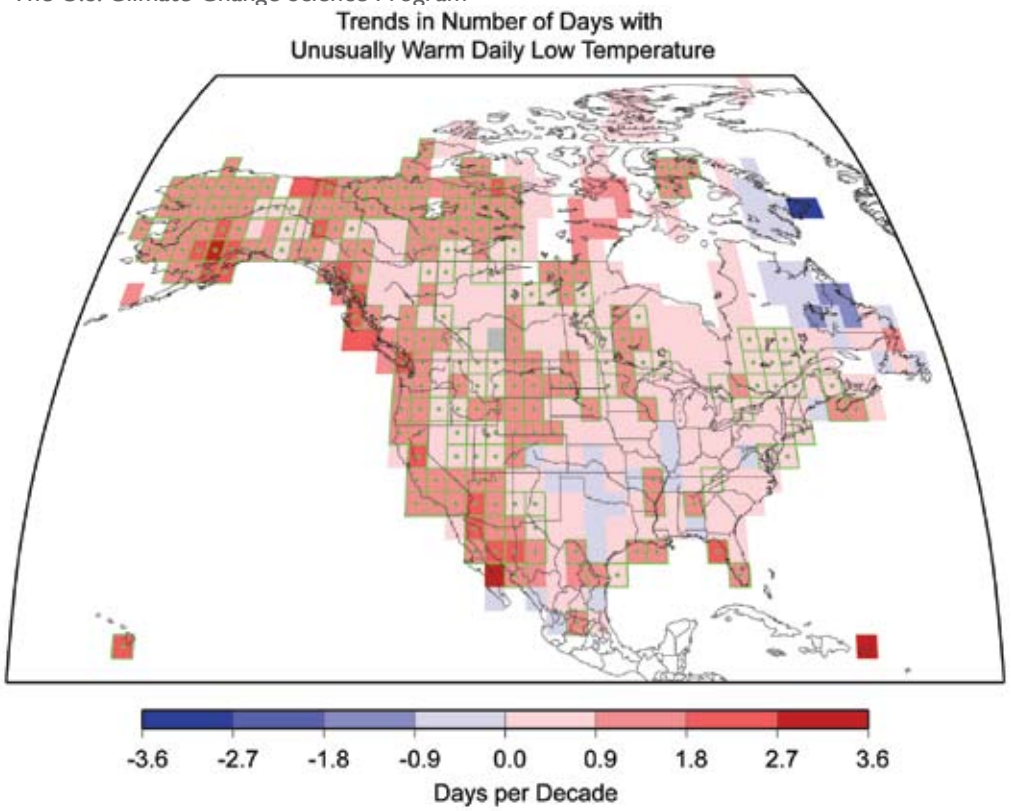


**Figure 2.2** Trends in the number of days in a year when the daily low is unusually warm (*i.e.*, in the top 10% of warm nights for the 1950-2004 period). Grid boxes with green squares are statistically significant at the p=0.05 level (Peterson *et al.*, 2008). A trend of 1.8 days/decade translates to a trend of 9.9 days over the entire 55 year (1950-2004) period, meaning that ten days more a year will have unusually warm nights.

There have been more rare heat events and fewer rare cold events in recent decades.

days to about 13% for maximum and almost 15% for minimum. These changes decrease as the threshold temperatures increase, indicating more rare events. The 97.5 percentage increases from about 3% of the days to 4% for maximum and 5% for minimum. The relative changes are similar. There are important regional differences in the changes. For example, the largest increases in the 90th percentile threshold temperature occur in the western part of the continent from northern Mexico through the western United States and Canada and across Alaska, while some areas, such as eastern Canada, show declines of as many as ten days per year from 1950 to 2004 (Figure 2.2).

Other regional studies have shown similar patterns of change. For the United States, the number of days exceeding the 90th, 95th and 99th percentile thresholds (defined monthly) have increased in recent years[3], but are also dominated earlier in the 20th century by the extreme heat and drought of the 1930s[4] (DeGaetano and Allen, 2002). Changes in cold extremes (days falling below the 10th, 5th, and 1st percentile threshold temperatures) show decreases, particularly since 1960[5]. For the 1900-1998 period in Canada, there are fewer cold extremes in winter, spring and summer in most of southern Canada and more high temperature extremes in winter and spring, but little change in high temperature extremes in summer[6] (Bonsal *et al.*, 2001). However, for the more recent (1950-1998) period there are significant increases in high temperature extremes over western Canada, but decreases in eastern Canada. Similar results averaged across all of Canada are found for the longer 1900-2003 period, with 28 fewer cold nights, 10 fewer cold days, 21 more extremely warm nights, and 8 more hot days per year now than in 1900[7] (Vincent and Mekis, 2006). For the United States and Canada, the largest increases in daily maximum and minimum temperature are occurring in the colder days of each month (Robeson, 2004). For the Caribbean region, there is an 8% increase in the number of very warm nights and 6% increase in the number of hot days for the 1958-1999 period. There also has been a corresponding decrease of 7% in the number of cold days and 4% in the number of cold nights (Peterson *et al.*, 2002). The number of very warm nights has increased by 10 or more per year for Hawaii and 15 or more per year for Puerto Rico from 1950 to 2004 (Figure 2.2).

[3] Stations with statistically significant upward trends for 1960-1996 passed tests for field significance based on resampling.

[4] The number of stations with statistically significant negative trends for 1930-1996 was greater than the number with positive trends.

[5] Stations with statistically significant downward trends for 1960-1996 passed tests for field significance based on resampling, but not for 1930-1996.

[6] Statistical significance of trends was assessed using Kendall's tau test.

[7] These trends were statistically significant at more than 20% of the stations based on Kendall's tau test.

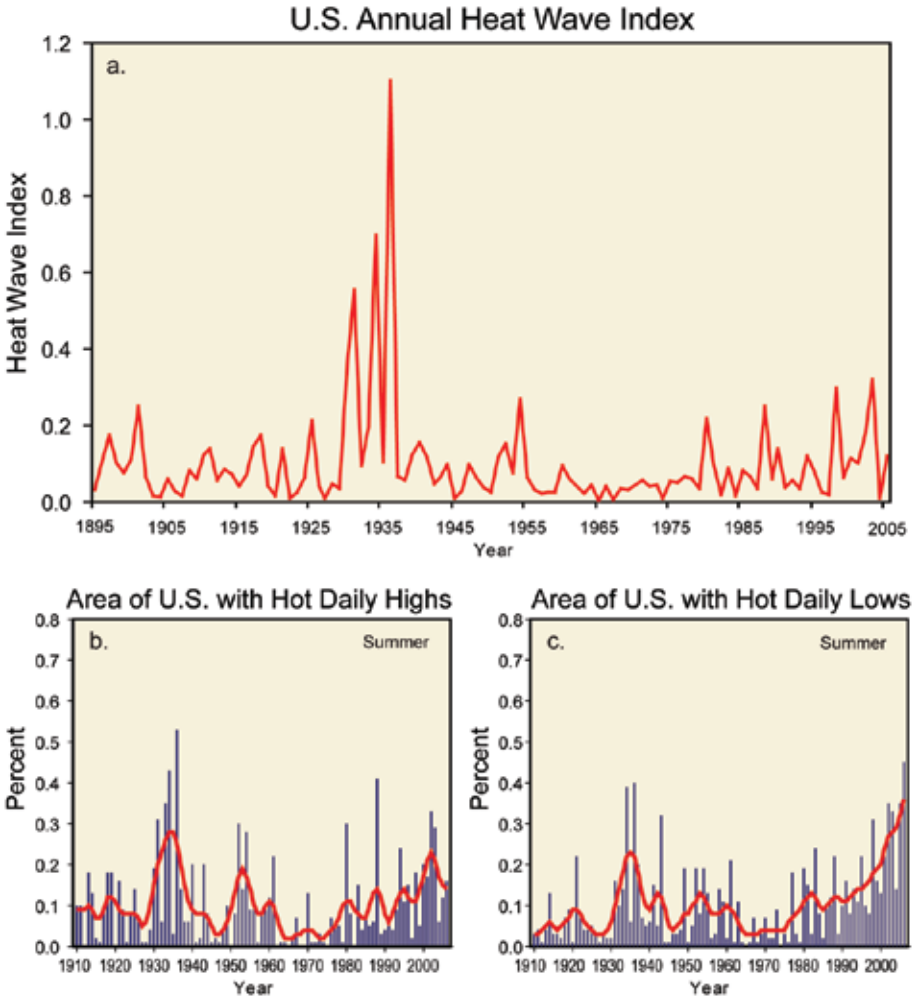


**Figure 2.3** Time series of (a) annual values of a U.S. national average "heat wave" index. Heat waves are defined as warm spells of 4 days in duration with mean temperature exceeding the threshold for a 1 in 10 year event. (updated from Kunkel *et al.,* 1999); (b)Area of the United States (in percent) with much above normal daily high temperatures in summer; (c) Area of the United States (in percent) with much above normal daily low temperatures in summer. Blue vertical bars give values for individual seasons while red lines are smoothed (9-year running) averages. The data used in (b) and (c) were adjusted to remove urban warming bias.

Analysis of multi-day very extreme heat and cold episodes[8] in the United States were updated[9] from Kunkel *et al.* (1999a) for the period 1895-2005. The most notable feature of the pattern of the annual number of extreme heat waves (Figure 2.3a) through time is the high frequency in the 1930s compared to the rest of the years in the 1895-2005 period. This was followed by a decrease to a minimum in the 1960s and 1970s and then an increasing trend since then. There is no trend over the entire period, but a highly statistically significant upward trend since 1960. The heat waves during the 1930s were characterized by extremely high daytime temperatures while nighttime temperatures were not as unusual (Figure 2.3b,c). An extended multi-year period of intense drought undoubtedly played a large role in the extreme heat of this period, particularly the daytime temperatures, by depleting soil moisture and reducing the moderating effects of evaporation. By contrast, the recent period of increasing heat wave index is distinguished by the dominant contribution of a rise in extremely high nighttime temperatures (Figure 2.3c). Cold waves show a decline in the first half of the 20th century, then a large spike of events during the mid-1980s, then a decline[10]. The last 10 years have seen a lower number of severe cold waves in the United States than in any other 10-year period since record-keeping began in 1895, consistent with observed impacts such as increasing insect populations (Chapter 1, Box 1.2). Decreases in the frequency of extremely low nighttime temperatures have made a somewhat greater contribution than extremely low daytime temperatures to this recent low period of cold waves. Over the entire period there is a downward trend, but it is not statistically significant at the p=0.05 level.

The annual number of warm spells[11] averaged over North America has increased since 1950 (Peterson *et al.*, 2008). The frequency and extent of hot summers[12] was highest in the 1930s, 1950s, and 1995-2003; the geographic

In contrast to the 1930s, the recent period of increasing heat wave index is distinguished by the dominant contribution of a rise in extremely high nighttime temperatures.

[8] The threshold is approximately the 99.9 percentile.

[9] The data were first transformed to create near-normal distributions using a log transformation for the heat wave index and a cube root transformation for the cold wave index. The transformed data were then subjected to least squares regression. Details are given in Appendix A, Example 2.

[10] Details of this analysis are given in Appendix A, Example 1.

[11] Defined as at least three consecutive days above the 90th percentile threshold done separately for maximum and minimum temperature.

[12] Based on percentage of North American grid points with summer temperatures above the 90th or below the 10th percentiles of the 1950-1999 summer climatology.

pattern of hot summers during 1995-2003 was similar to that of the 1930s (Gershunov and Douville, 2008).

For the U.S. as a whole, the average length of the frost-free season over the 1895-2000 period increased by almost two weeks.

The occurrence of temperatures below the biologically and societally important freezing threshold (0°C, 32°F) is an important aspect of the cold season climatology. Studies have typically characterized this either in terms of the number of frost days (days with the minimum temperature below freezing) or the length of the frost-free season[13]. The number of frost days decreased by four days per year in the United States during the 1948-1999 period, with the largest decreases, as many as 13 days per year, occurring in the western United States[14] (Easterling, 2002). In Canada, there have been significant decreases in frost day occurrence over the entire country from 1950 to 2003, with the largest decreases in extreme western Canada where there have been decreases of up to 40 or more frost days per year, and slightly smaller decreases in eastern Canada (Vincent and Mekis, 2006). The start of the frost-free season in the northeastern United States occurred 11 days earlier in the 1990s than in the 1950s (Cooter and LeDuc, 1995). For the U.S. as a whole, the average length of the frost-free season over the 1895-2000 period increased by almost two weeks[15] (Figure 2.4; Kunkel *et al.*, 2004). The change is characterized by four distinct regimes, with decreasing frost-free season length from 1895 to 1910, an increase in length of about one week from 1910 to 1930, little change during 1930-1980, and large increases since 1980. The frost-free season length has increased more in the western United States than in the eastern United States (Easterling, 2002; Kunkel *et al.*, 2004), which is consistent with the finding that the spring pulse of snow melt water in the Western United States now comes as much as 7-10 days earlier than in the late 1950s (Cayan *et al.*, 2001).

Ice cover on lakes and the oceans is a direct reflection of the number and intensity of cold, below freezing days. Ice cover on the Laurentian Great Lakes of North American usually forms along the shore and in shallow areas in December and January, and in deeper mid-lake areas in February due to their large depth and heat storage capacity. Ice loss usually starts in early to mid-March and lasts through mid- to late April (Assel, 2003).

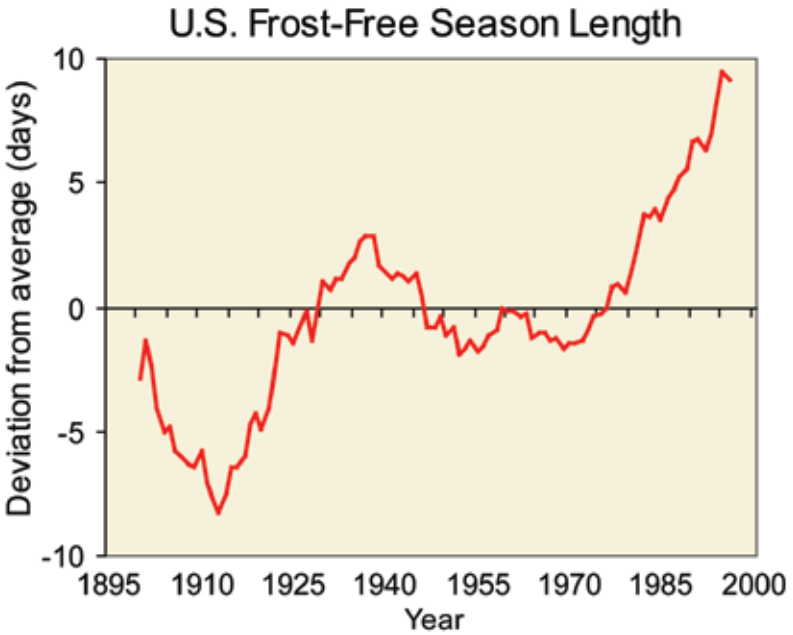


**Figure 2.4** Change in the length of the frost-free season averaged over the United States (from Kunkel *et al.*, 2003). The frost-free season is at least ten days longer on average than the long-term average.

Annual maximum ice cover on the Great Lakes has been monitored since 1963. The maximum extent of ice cover over the past four decades varied from less than 10% to over 90%. The winters of 1977-1982 were characterized by a higher ice cover regime relative to the prior 14 winters (1963-1976) and the following 24 winters (1983-2006) (Assel *et al.*, 2003; Assel, 2005a; Assel personal communication for winter 2006). A majority of the mildest winters with lowest seasonal average ice cover (Assel, 2005b) over the past four decades occurred during the most recent 10-year period (1997-2006). Analysis of ice breakup dates on other smaller lakes in North America with at least 100 years of data (Magnuson *et al.*, 2000) show a uniform trend toward earlier breakup dates (up to 13 days earlier per 100 years)[16].

[13] The difference between the date of the last spring frost and the first fall frost.

[14] Trends in the western half of the United States were statistically significant based on simple linear regression.

[15] Statistically significant based on least-squares linear regression.

[16] Statistically significant trends were found for 16 of 24 lakes.

Reductions in Arctic sea ice, especially near-shore sea ice, allow strong storm and wave activity to produce extensive coastal erosion resulting in extreme impacts. Observations from satellites starting in 1978 show that there has been a substantial decline in Arctic sea ice, with a statistically significant decreasing trend in annual Arctic sea ice extent of -33,000 (± 8,800) km$^2$ per year (equivalent to approximately -7% ± 2% since 1978). Seasonally the largest changes in Arctic sea ice have been observed in the ice that survives the summer, where the trend in the minimum Arctic sea ice extent, between 1979 and 2005, was -60,000 ± 24,000 km$^2$ per year (–20% ± 8%) (Lemke *et al.*, 2007). The 2007 summer sea-ice minimum was dramatically lower than the previous record low year of 2005.

Rising sea surface temperatures have led to an increase in the frequency of extreme high SST events causing coral bleaching (Box 1.1, Chapter 1). Mass bleaching events were not observed prior to 1980. However, since then, there have been six major global cycles of mass bleaching, with increasing frequency and intensity (Hoegh-Guldberg, 2005). Almost 30% of the world's coral reefs have died in that time.

Less scrutiny has been focused on Mexico temperature extremes, in part, because much of the country can be classified as a "tropical climate" where temperature changes are presumed fairly small, or semi-arid to arid climate where moisture availability exerts a far greater influence on human activities than does temperature.

Most of the sites in Mexico's oldest temperature observing network are located in major metropolitan areas, and there is considerable evidence to indicate that trends at least partly reflect urbanization and urban heat island influences (Englehart and Douglas, 2003). To avoid such issues in analysis, a monthly rural temperature data set has recently been developed[17]. Examined in broad terms as a national aggregate, a couple of basic behaviors emerge. First, long period temperature trends over Mexico are generally compatible with continental-scale trends which indicate a cooling trend over North America from about the mid-1940s to the mid-1970s, with a warming trend thereafter.

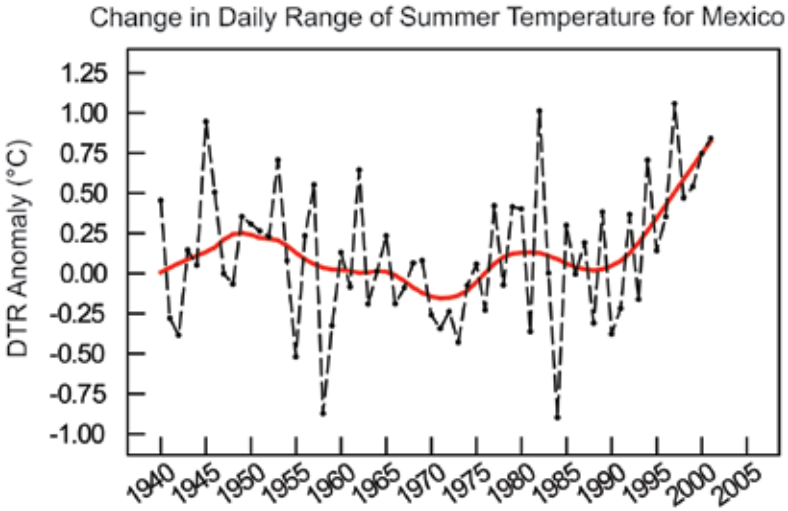


**Figure 2.5** Change in the daily range of temperature (difference between the daily low and the daily high temperature) during the warm season (June-Sept) for Mexico. This difference is known as a Diurnal Temperature Range (DTR). The recent rise in the daily temperature range reflects hotter daily summer highs. The time series represents the average DTR taken over the four temperature regions of Mexico as defined in Englehart and Douglas (2004). Trend line (red) based on LOWESS smoothing (*n*=30).

The rural gridded data set indicates that much of Mexico experienced decreases in both maximum daily temperature and minimum daily temperature during the 1941-1970 period (-0.8°C for maximum daily temperature and -0.6°C for minimum daily temperature), while the later period of 1971-2001 is dominated by upward trends that are most strongly evident in maximum daily temperature (1.1°C for maximum daily temperature and 0.3°C for minimum daily temperature). Based on these results, it appears very likely that much of Mexico has experienced an increase in average temperature driven in large measure by increases in maximum daily temperature. The diurnal temperature range (the difference between the daily high and the daily low temperature) for the warm season (June-September) averaged over all of Mexico has increased by 0.8°C since 1970, with particularly rapid rises since 1990 (Figure

There has been a substantial decline in arctic sea ice which allow strong storm and wave activity to produce extensive coastal erosion resulting in extreme impacts.

[17] It consists of monthly historical surface air temperature observations (1940-2001) compiled from stations (n=103) located in places with population <10,000 (2000 Census) and outside the immediate environment of large metropolitan areas. About 50% of the stations are located in places with <1000 inhabitants, and fewer than 10% of the stations are in places with >5000 population. To accommodate variable station record lengths and missing monthly observations, the data set is formatted as a grid-type (2.5° x 2.5° lat.-long.) based on the climate anomaly method (Jones and Moberg, 2003).

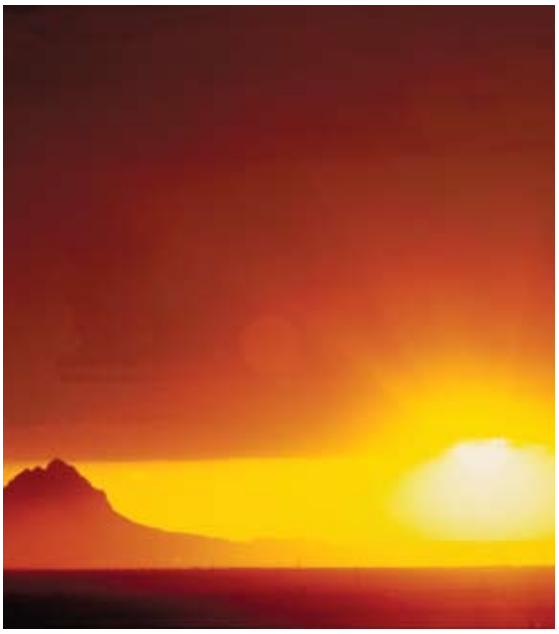

2.5), reflecting a comparatively rapid rise in maximum daily temperature with respect to minimum daily temperature (Englehart and Douglas, 2005)[18]. This behavior departs from the general picture for many regions of the world, where warming is attributable mainly to a faster rise in minimum daily temperature than in maximum daily temperature (*e.g.,* Easterling *et al.*, 1997). Englehart and Douglas (2005) indicate that the upward trend in diurnal temperature range for Mexico is in part a response to land use changes as reflected in population trends, animal numbers and rates of change in soil erosion.

Droughts are one of the most costly natural disasters, with estimated annual U.S. losses of $6–8 billion.

### 2.2.2 Precipitation Extremes

#### 2.2.2.1 Drought

Droughts are one of the most costly natural disasters (Chapter 1, Box 1.4), with estimated annual U.S. losses of $6–8 billion (Federal Emergency Management Agency, 1995). An extended period of deficient precipitation is the root cause of a drought episode, but the intensity can be exacerbated by high evaporation rates arising from excessive temperatures, high winds, lack of cloudiness, and/or low humidity. Drought can be defined in many ways, from acute short-term to chronic long-term hydrological drought, agricultural drought, meteorological drought, and so on. The assessment in this report focuses mainly on meteorological droughts based on the Palmer (1965) Drought Severity Index (PDSI), though other indices are also documented in the report (Chapter 2, Box 2.1).

Individual droughts can occur on a range of geographic scales, but they often affect large areas, and can persist for many months and even years. Thus, the aggregate impacts can be very large. For the United States, the percentage area affected by severe to extreme drought (Figure 2.6) highlights some major episodes of extended drought. The most widespread and severe drought conditions occurred in the 1930s and 1950s (Andreadis *et al.*, 2005). The early 2000s were also characterized by severe droughts in some areas, notably in the western United States. When averaged across the entire United States (Figure 2.6), there is no clear tendency for a trend based on the PDSI. Similarly, long-term trends (1925-2003) of hydrologic droughts based on model derived soil moisture and runoff show that droughts have, for the most part, become shorter, less frequent, and cover a smaller portion of the U. S. over the last century (Andreadis and Lettenmaier, 2006). The main exception is the Southwest and parts of the interior of the West, where increased temperature has led to rising drought trends (Groisman *et al.*, 2004; Andreadis and Lettenmaier, 2006). The trends averaged over all of North America since 1950 (Figure 2.6) are similar to U.S. trends for the same period, indicating no overall trend.

Since the contiguous United States has experienced an increase in both temperature and precipitation during the 20th century, one question is whether these increases are impacting the occurrence of drought. Easterling *et al.* (2007) examined this possibility by looking at drought, as defined by the PDSI, for the United States using detrended temperature and precipitation. Results indicate that without the upward trend

[18] Statistically significant trends were found in the northwest, central, and south, but not the northeast regions.

in precipitation, the increase in temperatures would have led to an increase in the area of the United States in severe-extreme drought of up to 30% in some months. However, it is most useful to look at drought in a regional context because as one area of the country is dry, often another is wet.

Summer conditions, which relate to fire danger, have trended toward lesser drought in the upper Mississippi, Midwest, and Northwest, but the fire danger has increased in the Southwest, in California in the spring season (not shown), and, surprisingly, over the Northeast, despite the fact that annual precipitation here has increased. A century-long warming in this region is quite significant in summer, which attenuates the precipitation contribution to soil wetness (Groisman *et al.*, 2004). Westerling *et al.* (2006) document that large wildfire activity in the western United States increased suddenly and markedly in the mid-1980s, with higher large-wildfire frequency, longer wildfire durations, and longer wildfire seasons. The greatest increases occurred in mid-elevation Northern Rockies forests, where land-use histories have relatively little effect on fire risks, and are strongly associated with increased spring and summer temperatures and an earlier spring snowmelt.

For the entire North American continent, there is a north-south pattern in drought trends (Dai *et al.*, 2004). Since 1950, there is a trend toward wetter conditions over much of the conterminous United States, but a trend toward drier conditions over southern and western Canada, Alaska, and Mexico. The summer PDSI averaged for Canada indicates dry conditions during the 1940s and 1950s, generally wet conditions from the 1960s to 1995, but much drier after 1995 (Shabbar and Skinner, 2004). In Alaska and Canada, the upward trend in temperature, resulting in increased evaporation rates, has made a substantial contribution to the upward trend in drought (Dai *et al.*, 2004). In agreement with this drought index analysis, the area of forest fires in Canada has been quite high since 1980 compared to the previous 30 years, and Alaska experienced a record high year for forest fires in 2004 followed by the third highest in 2005 (Soja *et al.*, 2007). During the mid-1990s and early 2000s, central and western Mexico (Kim *et al.*, 2002; Nicholas and Battisti, 2008; Hallack-Alegria and Watkins, 2007) experienced continuous cool-season droughts having major impacts in agriculture, forestry, and ranching, especially during the warm summer season. In 1998, "El Niño" caused one of the most severe droughts in Mexico since the 1950s (Ropelewski, 1999), creating the worst wildfire season in Mexico's history. Mexico had 14,445 wildfires affecting 849,632 hectares–the largest area ever burned in Mexico in a single season (SEMARNAT, 2000).

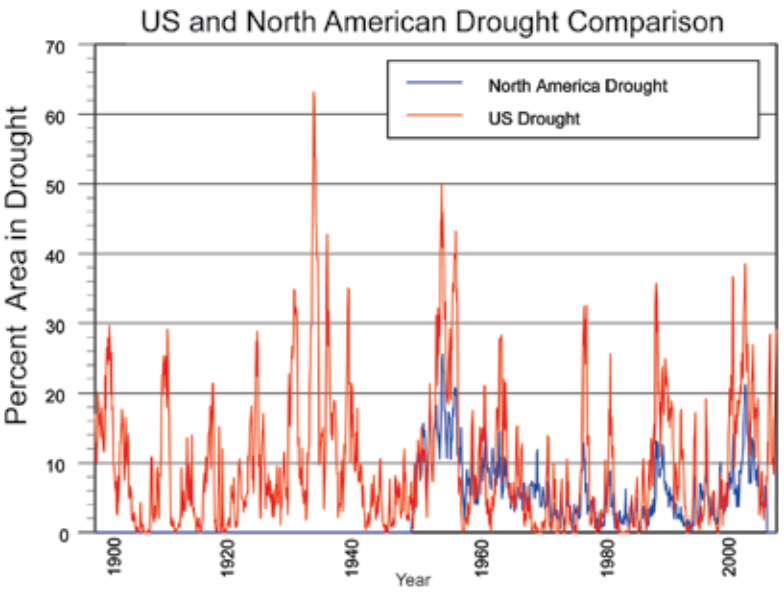


**Figure 2.6** The area (in percent) of area in severe to extreme drought as measured by the Palmer Drought Severity Index for the United States (red) from 1900 to present and for North America (blue) from 1950 to present.

The greatest increases in wildfire activity have occurred in mid-elevation Northern Rockies forests, and are strongly associated with increased spring and summer temperatures and earlier spring snowmelt.

Reconstructions of drought prior to the instrumental record based on tree-ring chronologies indicate that the 1930s may have been the worst drought since 1700 (Cook *et al.*, 1999). There were three major multiyear droughts in the United States during the latter half of the 1800s: 1856-1865, 1870-1877, and 1890-1896 (Herweijer *et al.*, 2006). Similar droughts have been reconstructed for northern Mexico (Therrell *et al.*, 2002). There is evidence of earlier, even more intense drought episodes (Woodhouse and Overpeck, 1998). A period in the mid- to late 1500s has been termed a "mega-drought" and was longer-lasting and more widespread than the 1930s Dust Bowl (Stahle *et al.*, 2000). Several additional mega-droughts occurred during the years 1000-1470 (Herweijer *et al.*, 2007). These droughts were about as severe as the 1930s Dust

## BOX 2.1: "Measuring" Drought

Drought is complex and can be "measured" in a variety of ways. The following list of drought indicators are all based on commonly-observed weather variables and fixed values of soil and vegetation properties. Their typical application has been for characterization of past and present drought intensity. For use in future projections of drought, the same set of vegetation properties is normally used. However, some properties may change. For example, it is known that plant water use efficiency increases with increased $CO_2$ concentrations. There have been few studies of the magnitude of this effect in realistic field conditions. A recent field study (Bernacchi *et al.*, 2007) of the effect of $CO_2$ enrichment on evapotranspiration (ET) from unirrigated soybeans indicated an ET decrease in the range of 9-16% for $CO_2$ concentrations of 550 parts per million (ppm) compared to present-day $CO_2$ levels. Studies in native grassland indicated plant water use efficiency can increase from 33% - 69% under 700-720 ppm $CO_2$ (depending on species). The studies also show a small increase in soil water content of less than 20% early on (Nelson *et al.*, 2004), which disappeared after 50 days in one experiment (Morgan *et al.*, 1998), and after 3 years in the other (Ferretti *et al.*, 2003). These experiments over soybeans and grassland suggest that the use of existing drought indicators without any adjustment for consideration of $CO_2$ enrichment would tend to have a small overestimate of drought intensity and frequency, but present estimates indicate that it is an order of magnitude smaller effect, compared to traditional weather and climate variations. Another potentially important effect is the shift of whole biomes from one vegetation type to another. This could have substantial effects on ET over large spatial scales (Chapin *et al.*, 1997).

- **Palmer Drought Severity Index (PDSI; Palmer, 1965)** – meteorological drought. The PDSI is a commonly used drought index that measures intensity, duration, and spatial extent of drought. It is derived from measurements of precipitation, air temperature, and local estimated soil moisture content. Categories range from less than -4 (extreme drought) to more than +4 (extreme wet conditions), and have been standardized to facilitate comparisons from region to region. Alley (1984) identified some positive characteristics of the PDSI that contribute to its popularity: (1) it is an internationally recognized index; (2) it provides decision makers with a measurement of the abnormality of recent weather for a region; (3) it provides an opportunity to place current conditions in historical perspective; and (4) it provides spatial and temporal representations of historical droughts. However, the PDSI has some limitations: (1) it may lag emerging droughts by several months; (2) it is less well suited for mountainous land or areas of frequent climatic extremes; (3) it does not take into account streamflow, lake and reservoir levels, and other long-term hydrologic impacts (Karl and Knight, 1985), such as snowfall and snow cover; (4) the use of temperature alone to estimate potential evapotranspiration (PET) can introduce biases in trend estimates because humidity, wind, and radiation also affect PET, and changes in these elements are not accounted for.
- **Crop Moisture Index (CMI; Palmer, 1968)** – short-term meteorological drought. Whereas the PDSI monitors long-term meteorological wet and dry spells, the CMI was designed to evaluate short-term moisture conditions across major crop-producing regions. It is based on the mean temperature and total precipitation for each week, as well as the CMI value from the previous week. Categories range from less than -3 (severely dry) to more than +3 (excessively wet). The CMI responds rapidly to changing conditions, and it is weighted by location and time so that maps, which commonly display the weekly CMI across the United States, can be used to compare moisture conditions at different

Bowl episode but much longer, lasting 20 to 40 years. In the western United States, the period of 900-1300 was characterized by widespread drought conditions (Figure 2.7; Cook *et al.*, 2004). In Mexico, reconstructions of seasonal precipitation (Stahle *et al.*, 2000, Acuña-Soto *et al.*, 2002, Cleaveland *et al.*, 2004) indicate that there have been droughts more severe than the 1950s drought, *e.g.*, the mega-drought in the mid- to late-16th century, which appears as a continental-scale drought.

During the summer months, excessive heat and drought often occur simultaneously because the meteorological conditions typically causing drought are also conducive to high temperatures. The impacts of the Dust Bowl droughts and the 1988 drought were compounded by

locations. Weekly maps of the CMI are available as part of the USDA/JAWF Weekly Weather and Crop Bulletin.

- **Standardized Precipitation Index (SPI; McKee *et al.*, 1993)** – precipitation-based drought. The SPI was developed to categorize rainfall as a standardized departure with respect to a rainfall probability distribution function; categories range from less than -3 (extremely dry) to more than +3 (extremely wet). The SPI is calculated on the basis of selected periods of time (typically from 1 to 48 months of total precipitation), and it indicates how the precipitation for a specific period compares with the long-term record at a given location (Edwards and McKee, 1997). The index correlates well with other drought indices. Sims *et al.* (2002) suggested that the SPI was more representative of short-term precipitation and a better indicator of soil wetness than the PDSI. The 9-month SPI corresponds closely to the PDSI (Heim, 2002; Guttman, 1998).
- **Keetch-Byram Drought Index (KBDI; Keetch and Byram, 1968)** – meteorological drought and wildfire potential index. This was developed to characterize the level of potential fire danger. It uses daily temperature and precipitation information and estimates soil moisture deficiency. High values of KBDI are indicative of favorable conditions for wildfires. However, the index needs to be regionalized, as values are not comparable among regions (Groisman *et al.*, 2004, 2007).
- **No-rain episodes** – meteorological drought. Groisman and Knight (2007, 2008) proposed to directly monitor frequency and intensity of prolonged no-rain episodes (greater than 20, 30, 60, *etc.* days) during the warm season, when evaporation and transpiration are highest and the absence of rain may affect natural ecosystems and agriculture. They found that during the past four decades the duration of prolonged dry episodes has significantly increased over the eastern and southwestern United States and adjacent areas of northern Mexico and southeastern Canada.
- **Soil Moisture and Runoff Index (SMRI; Andreadis and Lettenmaier, 2006)**–hydrologic and agricultural droughts. The SMRI is based on model-derived soil moisture and runoff as drought indicators; it uses percentiles and the values are normalized from 0 (dry) to 1 (wet conditions). The limitation of this index is that it is based on land-surface model-derived soil moisture. However, long-term records of soil moisture – a key variable related to drought – are essentially nonexistent (Andreadis and Lettenmaier, 2006). Thus, the advantage of the SMRI is that it is physically based and with the current sophisticated land-surface models it is easy to produce multimodel average climatologies and century-long reconstructions of land surface conditions, which could be compared under drought conditions.

*Resources:* A list of these and other drought indicators, data availability, and current drought conditions based on observational data can be found at NOAA's National Climatic Data Center (NCDC, http://www.ncdc.noaa.gov). The North American Drought Monitor at NCDC monitors current drought conditions in Canada, the United States, and Mexico. Tree-ring reconstruction of PDSI across North America over the last 2000 years can be also found at NCDC.

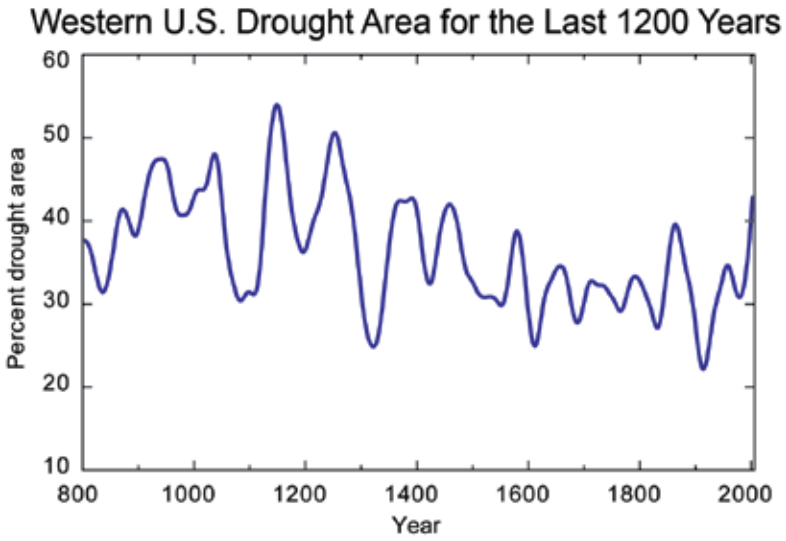


**Figure 2.7** Area of drought in the western United States as reconstructed from tree rings (Cook *et al.,* 2004).

episodes of extremely high temperatures. The month of July 1936 in the central United States is a notable example. To illustrate, Lincoln, NE received only 0.05" of precipitation that month (after receiving less than 1 inch the previous month) while experiencing temperatures reaching or exceeding 110°F on 10 days, including 117°F on July 24. Although no studies of trends in such "compound" extreme events have been performed, they represent a significant societal risk.

#### 2.2.2.2 Short Duration Heavy Precipitation

##### *2.2.2.2.1 Data Considerations and Terms*

One of the clearest trends in the U.S. observational record is an increasing frequency and intensity of heavy precipitation events.

Intense precipitation often exhibits higher geographic variability than many other extreme phenomena. This poses challenges for the analysis of observed data since the heaviest area of precipitation in many events may fall between stations. This adds uncertainty to estimates of regional trends based on the climate network. The uncertainty issue is explicitly addressed in some recent studies.

Precipitation extremes are typically defined based on the frequency of occurrence (by percentile [*e.g.*, upper 5%, 1%, 0.1%, *etc.*] or by return period [*e.g.*, an average occurrence of once every 5 years, once every 20 years, *etc.*]), and/or their absolute values (*e.g.*, above 50 mm, 100 mm, 150 mm, or more). Values of percentile or return period thresholds vary considerably across North America. For example, in the United States, regional average values of the 99.9 percentile threshold for daily precipitation are lowest in the Northwest and Southwest (average of 55 mm) and highest in the South (average of 130mm)[19].

As noted above, spatial patterns of precipitation have smaller spatial correlation scales (for example, compared to temperature and atmospheric pressure) which means that a denser network is required in order to achieve a given uncertainty level. While monthly precipitation time series for flat terrain have typical radii of correlation[20] (ρ) of approximately 300 km or even more, daily precipitation may have ρ less than 100 km with typical values for convective rainfall in isolated thunderstorms of approximately 15 to 30 km (Gandin and Kagan, 1976). Values of ρ can be very small for extreme rainfall events, and sparse networks may not be adequate to detect a desired minimum magnitude of change that can result in societally-important impacts and can indicate important changes in the climate system.

##### *2.2.2.2.2 United States*

One of the clearest trends in the United States observational record is an increasing frequency and intensity of heavy precipitation events (Karl and Knight, 1998; Groisman *et al.*, 1999, 2001, 2004, 2005; Kunkel *et al.*, 1999b; Easterling *et al.*, 2000; IPCC, 2001; Semenov and Bengtsson, 2002; Kunkel, 2003). One measure of this is how much of the annual precipitation at a location comes from days with precipitation exceeding 50.8 mm (2 inches) (Karl and Knight, 1998). The area of the United States affected by a much above normal contribution from these heavy precipitation days increased by a statistically significant amount, from about 9% in the 1910s to about 11% in the 1980s and 1990s (Karl and Knight, 1998). Total precipitation also increased during this time, due in large part to increases in the intensity of heavy precipitation events (Karl and Knight, 1998). In

[19] The large magnitude of these differences is a major motivation for the use of regionally-varying thresholds based on percentiles.

[20] Spatial correlation decay with distance, r, for many meteorological variables, X, can be approximated by an exponential function of distance: Corr (X(A), X(B)) ~ $e^{-r/\rho}$ where r is a distance between point A and B and ρ is a radius of correlation, which is a distance where the correlation between the points is reduced to 1/e compared to an initial "zero" distance.

fact, there has been little change or decrease in the frequency of light and average precipitation days (Easterling *et al.*, 2000; Groisman *et al.*, 2004, 2005) during the last 30 years, while heavy precipitation frequencies have increased (Sun and Groisman, 2004). For example, the amount of precipitation falling in the heaviest 1% of rain events increased by 20% during the 20th century, while total precipitation increased by 7% (Groisman *et al.*, 2004). Although the exact character of those changes has been questioned (*e.g.*, Michaels *et al.*, 2004), it is highly likely that in recent decades extreme precipitation events have increased more than light to medium events.

Over the last century there was a 50% increase in the frequency of days with precipitation over 101.6 mm (four inches) in the upper midwestern U.S.; this trend is statistically significant (Groisman *et al.*, 2001). Upward trends in the amount of precipitation occurring in the upper 0.3% of daily precipitation events are statistically significant for the period of 1908-2002 within three major regions (the South, Midwest, and Upper Mississippi; Figure 2.8) of the central United States (Groisman *et al.*, 2004, 2005). The upward trends are primarily a warm season phenomenon when the most intense rainfall events typically occur. A time series of the frequency of events in the upper 0.3% averaged for these 3 regions (Fig 2.8) shows a 20% increase over the period of 1893-2002 with all of this increase occurring over the last third of the 1900s (Groisman *et al.*, 2005).

Examination of intense precipitation events defined by return period, covering the period

The amount of precipitation falling in the heaviest 1% of rain events increased by 20% during the 20th century, while total precipitation increased by 7%.

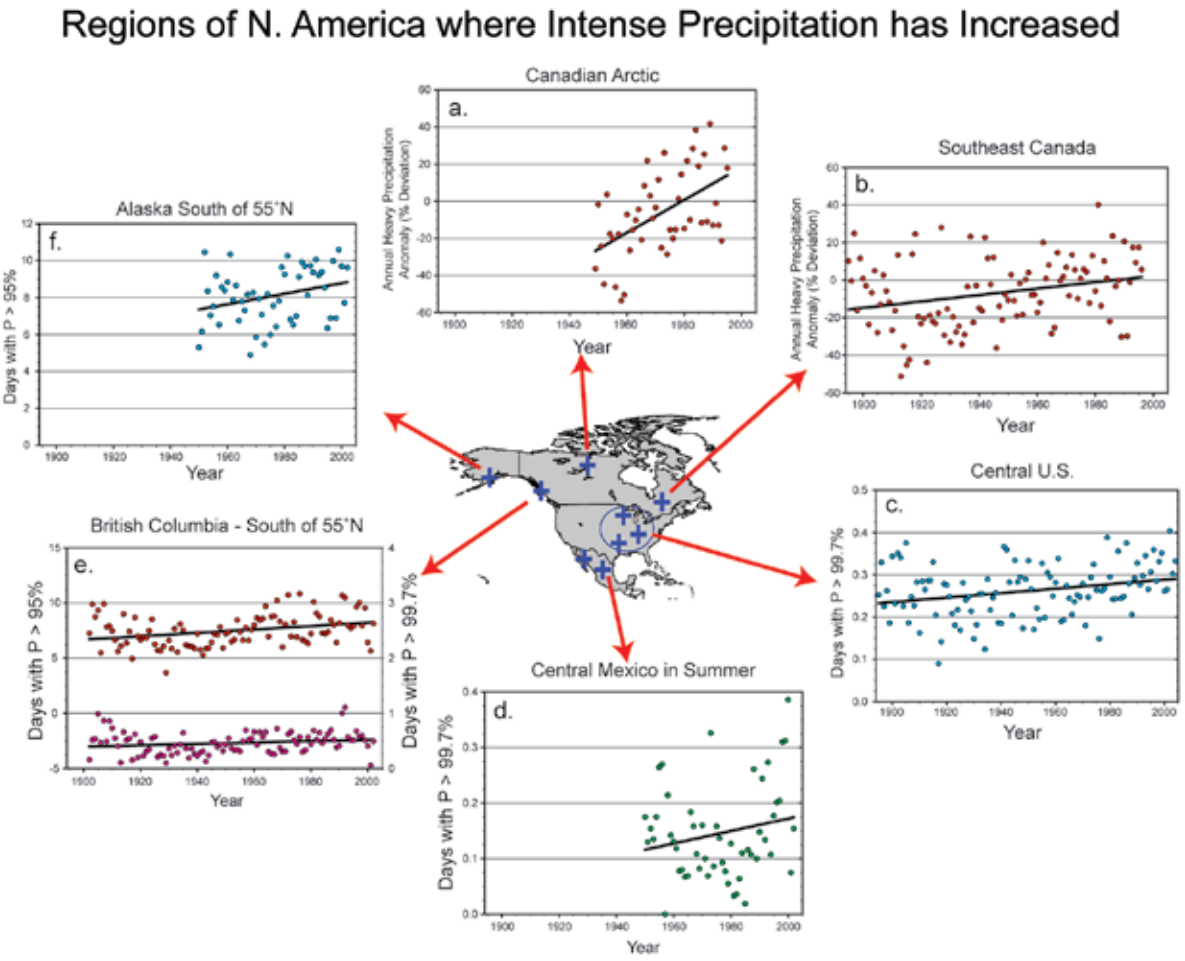


**Figure 2.8** Regions where disproportionate increases in heavy precipitation during the past decades were documented compared to the change in the annual and/or seasonal precipitation. Because these results come from different studies, the definitions of heavy precipitation vary. (a) annual anomalies (% departures) of heavy precipitation for northern Canada (updated from Stone *et al.,* 2000); (b) as (a), but for southeastern Canada; (c) the top 0.3% of daily rain events over the central United States and the trend (22%/113 years) (updated from Groisman *et al.,* 2005); (d) as for (c), but for southern Mexico; (e) upper 5%, top points, and upper 0.3%, bottom points, of daily precipitation events and linear trends for British Columbia south of 55°N; (f) upper 5% of daily precipitation events and linear trend for Alaska south of 62°N.

of 1895-2000, indicates that the frequencies of extreme precipitation events before 1920 were generally above the long-term averages for durations of 1 to 30 days and return periods 1 to 20 years, and only slightly lower than values during the 1980s and 1990s (Kunkel *et al.*, 2003). The highest values occur after about 1980, but the elevated levels prior to about 1920 are an interesting feature suggesting that there is considerable variability in the occurrence of extreme precipitation on decade-to-decade time scales

There is a seeming discrepancy between the results for the 99.7th percentile (which do not show high values early in the record in the analysis of Groisman *et al.*, 2004), and for 1 to 20-year return periods (which do show high values in the analysis of Kunkel *et al.*, 2003). The number of stations with available data is only about half (about 400) in the late 1800s of what is available in most of the 1900s (800-900). Furthermore, the geographic distribution of stations throughout the record is not uniform; the density in the western United States is relatively lower than in the central and eastern United States. It is possible that the resulting uncertainties in heavy precipitation estimates are too large to make unambiguous statements about the recent high frequencies.

It is highly likely that the recent elevated frequencies in heavy precipitation in the United States are the highest on record.

Recently, this question was addressed (Kunkel *et al.*, 2007a) by analyzing the modern dense network to determine how the density of stations affects the uncertainty, and then to estimate the level of uncertainty in the estimates of frequencies in the actual (sparse) network used in the long-term studies. The results were unambiguous. For all combinations of three precipitation durations (1-day, 5-day and 10-day) and three return periods (1-year, 5-year, and 20-year), the frequencies for 1983-2004 were significantly higher than those for 1895-1916 at a high level of confidence. In addition, the observed linear trends were all found to be upward, again with a high level of confidence. Based on these results, it is highly likely that the recent elevated frequencies in heavy precipitation in the United States are the highest on record.

#### *2.2.2.2.3 Alaska and Canada*

The sparse network of long-term stations in Canada increases the uncertainty in estimates of extremes. Changes in the frequency of heavy precipitation events exhibit considerable decade-to-decade variability since 1900, but no long-term trend for the century as a whole (Zhang *et al.*, 2001). However, according to Zhang *et al.* (2001), there are not sufficient instrumental data to discuss the nationwide trends in precipitation extremes over Canada prior to 1950. Nevertheless, there are changes that are noteworthy. For example, the frequency of the upper 0.3% of events exhibits a statistically significant upward trend of 35% in British Columbia since 1910 (Figure 2.8; Groisman *et al.*, 2005). For Canada, increases in precipitation intensity during the second half of the 1900s are concentrated in heavy and intermediate events, with the largest changes occurring in Arctic areas (Stone *et al.*, 2000). The tendency for increases in the frequency of intense precipitation, while the frequency of days with average and light precipitation does not change or decreases, has also been observed in Canada over the last 30 years (Stone *et al.*, 2000),

mirroring United States changes. Recently, Vincent and Mekis (2006) repeated analyses of precipitation extremes for the second half of the 1900s (1950-2003 period). They reported a statistically significant increase of 1.8 days over the period in heavy precipitation days (defined as the days with precipitation above 10 mm) and statistically insignificant increases in the maximum 5-day precipitation (by approximately 5%) and in the number of "very wet days" (defined as days with precipitation above the upper 5th percentiles of local daily precipitation [by 0.4 days]).

There is an upward trend of 39% in southern Alaska since 1950, although this trend is not statistically significant (Figure 2.8; Groisman *et al.*, 2005).

#### *2.2.2.2.4 Mexico*

On an annual basis, the number of heavy precipitation (P > 10 mm) days has increased in northern Mexico and the Sierra Madre Occidental and decreased in the south-central part of the country (Alexander *et al.*, 2006). The percent contribution to total precipitation from heavy precipitation events exceeding the 95th percentile threshold has increased in the monsoon region (Alexander *et al.*, 2006) and along the southern Pacific coast (Aguilar *et al.*, 2005), while some decreases are documented for south-central Mexico (Aguilar *et al.*, 2005).

On a seasonal basis, the maximum precipitation reported in five consecutive days during winter and spring has increased in northern Mexico and decreased in south-central Mexico (Alexander *et al.*, 2006). Northern Baja California, the only region in Mexico characterized by a Mediterranean climate, has experienced an increasing trend in winter precipitation exceeding the 90th percentile, especially after 1977 (Cavazos and Rivas, 2004). Heavy winter precipitation in this region is significantly correlated with El Niño events (Pavia and Badan, 1998; Cavazos and Rivas, 2004); similar results have been documented for California (*e.g.*, Gershunov and Cayan, 2003). During the summer, there has been a general increase of 2.5 mm in the maximum five-consecutive-day precipitation in most of the country, and an upward trend in the intensity of events exceeding the 99th and 99.7th percentiles in the high plains of northern Mexico during the summer season (Groisman *et al.,* 2005).

During the monsoon season (June-September) in northwestern Mexico, the frequency of heavy events does not show a significant trend (Englehart and Douglas, 2001; Neelin *et al.*, 2006). Similarly, Groisman *et al.* (2005) report that the frequency of very heavy summer precipitation events (above the 99th percentile) in the high plains of Northern Mexico (east of the core monsoon) has not increased, whereas their intensity has increased significantly.

The increase in the mean intensity of heavy summer precipitation events in the core monsoon region during the 1977-2003 period are significantly correlated with the Oceanic El Niño Index[21] conditions during the cool season. El Niño SST anomalies antecedent to the monsoon season are associated with less frequent, but more intense, heavy precipitation events[22] (exceeding the 95th percentile threshold), and vice versa.

There has been an insignificant decrease in the number of consecutive dry days in northern Mexico, while an increase is reported for south-central Mexico (Alexander *et al.*, 2006), and the southern Pacific coast (Aguilar *et al.*, 2005).

#### *2.2.2.2.5 Summary*

All studies indicate that changes in heavy precipitation frequencies are *always* higher than changes in precipitation totals and, in some regions, an *increase* in heavy and/or very heavy precipitation occurred while no change or even a decrease in precipitation totals was observed (*e.g.*, in the summer season in central Mexico). There are regional variations in which these changes are statistically significant (Figure 2.8). The most significant changes occur in the central United States; central Mexico; southeastern, northern, and western Canada; and

Changes in heavy precipitation frequencies are always higher than changes in precipitation totals, and in some regions, an increase in heavy and/or very heavy precipitation occurred while no change or even a decrease in precipitation totals was observed.

[21] Oceanic El Niño Index:http://www.cpc.ncep.noaa.gov/products/analysis_monitoring/ensostuff/ensoyears.shtml
Warm and cold episodes based on a threshold of +/- 0.5°C for the oceanic El Niño Index [3 month running mean of ERSST.v2 SST anomalies in the Niño 3.4 region (5°N-5°S, 120°-170°W)], based on the 1971-2000 base period.

[22] The correlation coefficient between oceanic El Niño Index and heavy precipitation frequency (intensity) is -0.37 (+0.46).

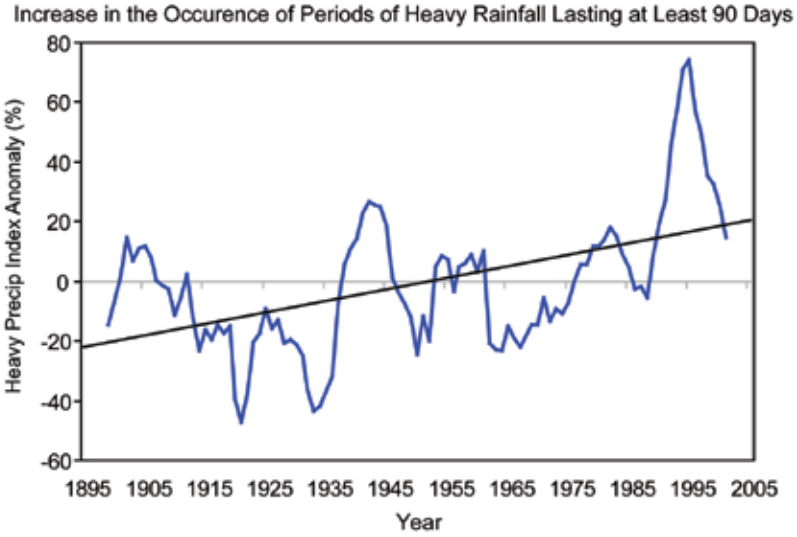


**Figure 2.9** Frequency (expressed as a percentage anomaly from the period of record average) of excessive precipitation periods of 90 day duration exceeding a 1-in-20-year event threshold for the U.S. The periods are identified from a time series of 90-day running means of daily precipitation totals. The largest 90-day running means were identified and these events were counted in the year of the first day of the 90-day period. Annual frequency values have been smoothed with a 9-yr running average filter. The black line shows the trend (a linear fit) for the annual values.

southern Alaska. These changes have resulted in a wide range of impacts, including human health impacts (Chapter 1, Box 1.3).

#### 2.2.2.3 Monthly to Seasonal Heavy Precipitation

On the main stems of large river basins, significant flooding will not occur from short duration extreme precipitation episodes alone. Rather, excessive precipitation must be sustained for weeks to months. The 1993 Mississippi River flood, which resulted in an estimated $17 billion in damages, was caused by several months of anomalously high precipitation (Kunkel *et al.*, 1994).

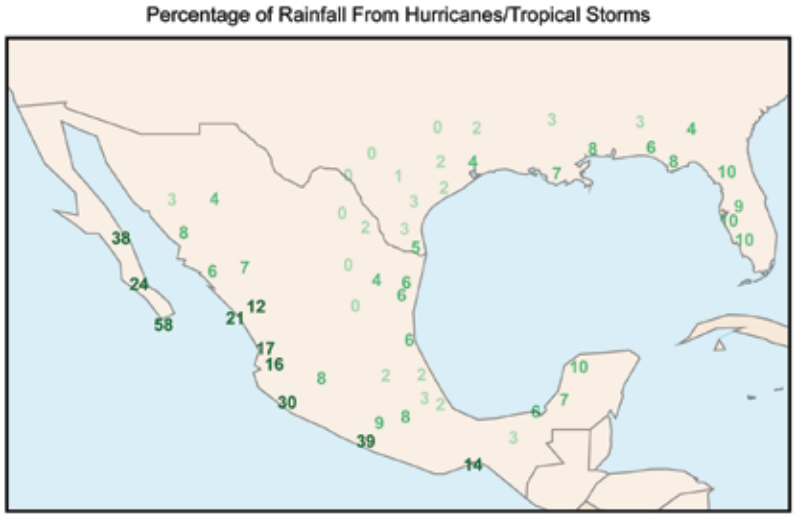


**Figure 2.10** Average (median) percentage of warm season rainfall (May-November) from hurricanes and tropical storms affecting Mexico and the Gulf Coast of the United States. Figure updated from Englehart and Douglas (2001).

A time series of the frequency of 90-day precipitation totals exceeding the 20-year return period (a simple extension of the approach of Kunkel *et al.*, 2003) indicates a statistically significant upward trend (Figure 2.9). The frequency of such events during the last 25 years is 20% higher than during any earlier 25-year period. Even though the causes of multi-month excessive precipitation are not necessarily the same as for short duration extremes, both show moderately high frequencies in the early 20th century, low values in the 1920s and 1930s, and the highest values in the past two to three decades. The trend[23] over the entire period is highly statistically significant.

#### 2.2.2.4 North American Monsoon

Much of Mexico is dominated by a monsoon type climate with a pronounced peak in rainfall during the summer (June through September) when up to 60% to 80% of the annual rainfall is received (Douglas *et al.*, 1993; Higgins *et al.*, 1999; Cavazos *et al.*, 2002). Monsoon rainfall in southwest Mexico is often supplemented by tropical cyclones moving along the coast. Farther removed from the tracks of Pacific tropical cyclones, interior and northwest sections of Mexico receive less than 10% of the summer rainfall from passing tropical cyclones (Figure 2.10; Englehart and Douglas, 2001). The main influences on total monsoon rainfall in these regions rests in the behavior of the monsoon as defined by its start and end date, rainfall intensity, and duration of wet and dry spells (Englehart and Douglas, 2006). Extremes in any one of these parameters can have a strong effect on the total monsoon rainfall.

The monsoon in northwest Mexico has been studied in detail because of its singular importance to that region, and because summer rainfall from this core monsoon region spills over into the United States Desert Southwest (Douglas *et al.*, 1993; Higgins *et al.,* 1999; Cavazos *et al.*, 2002). Based on long term data

[23] The data were first subjected to a square root transformation to produce a data set with an approximate normal distribution, then least squares regression was applied. Details can be found in Appendix A, Example 4.

from eight stations in southern Sonora, the summer rains have become increasingly late in arriving (Englehart and Douglas, 2006), and this has had strong hydrologic and ecologic repercussions for this northwest core region of the monsoon. Based on linear trend, the mean start date for the monsoon has been delayed almost 10 days (9.89 days with a significant trend of 1.57 days per decade) over the past 63 years (Figure 2.11a). Because extended periods of intense heat and desiccation typically precede the arrival of the monsoon, the trend toward later starts to the monsoon will place additional stress on the water resources and ecology of the region if continued into the future.

Accompanying the tendency for later monsoon starts, there also has been a notable change in the "consistency" of the monsoon as indicated by the average duration of wet spells in southern Sonora (Figure 2.11b). Based on a linear trend, the average wet spell[24] has decreased by almost one day (0.88 days with a significant trend of -0.14 days per decade) from nearly four days in the early 1940s to slightly more than three days in recent years. The decrease in wet spell length indicates a more erratic monsoon is now being observed. Extended periods of consecutive days with rainfall are now becoming less common during the monsoon. These changes can have profound influences on surface soil moisture levels which affect both plant growth and runoff in the region.

A final measure of long-term change in monsoon activity is associated with the change in rainfall intensity over the past 63 years (Figure 2.11c). Based on linear trend, rainfall intensity[25] in the 1940s was roughly 5.6 mm per rain day, but in recent years has risen to nearly 7.5 mm per rain day[26]. Thus, while the summer monsoon has become increasingly late in arriving and wet spells have become shorter, the average rainfall during rain events has actually increased very significantly by 17% or 1.89 mm over the 63 year period (0.3 mm per decade) as well as the intensity of heavy precipitation events (Figure 2.9). Taken together, these statistics indicate that rainfall in the core region of the monsoon (*i.e.*, northwest Mexico) has become more erratic with a tendency towards high intensity rainfall events, a shorter monsoon, and shorter wet spells.

Variability in Mexican monsoon rainfall shows modulation by large-scale climate modes. Englehart and Douglas (2002) demonstrate that a well-developed inverse relationship exists between ENSO and total seasonal rainfall (June-September) over much of Mexico, but the relationship is only operable in the positive phase of the PDO. Evaluating monsoon rainfall behavior on intraseasonal time scales, Englehart and Douglas (2006) demonstrate that rainfall intensity (mm per rain day) in the core region of the monsoon is related to PDO phase, with the positive (negative) phase favoring relatively high (low) intensity rainfall events. Analysis indicates that other rainfall characteristics of

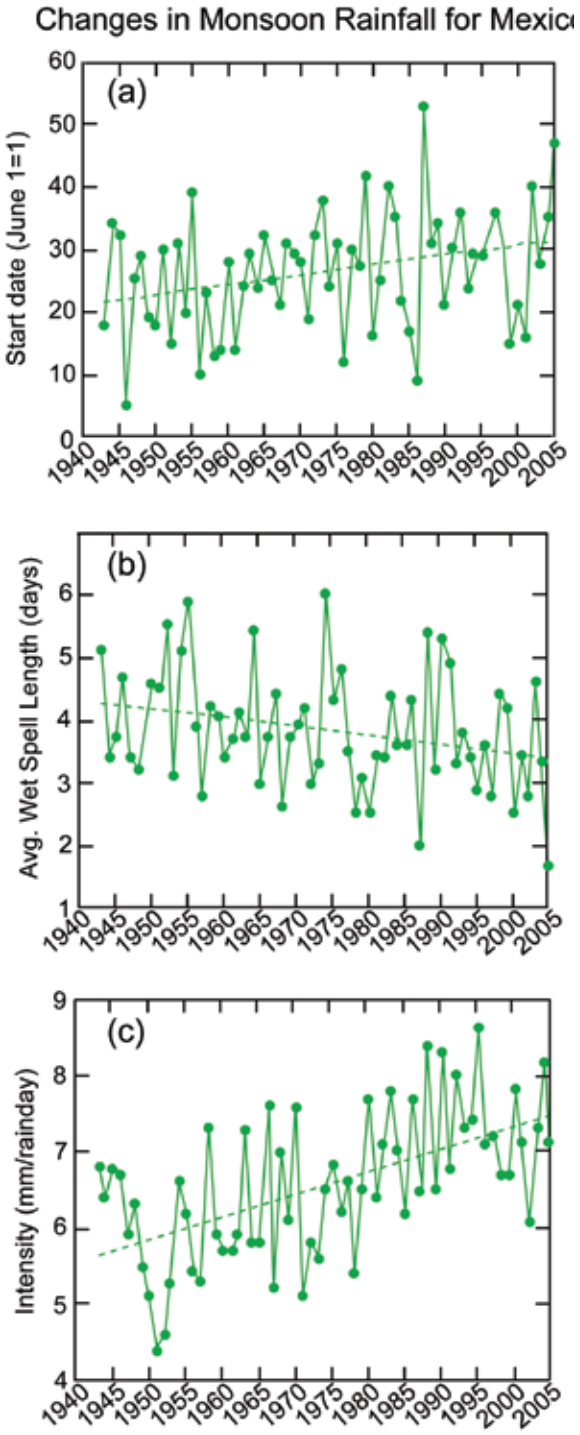


**Figure 2.11** Variations and linear trend in various characteristics of the summer monsoon in southern Sonora, Mexico; including: (a) the mean start date June 1 = Day 1 on the graph; (b) the mean wet spell length defined as the mean number of consecutive days with mean regional precipitation >1 mm; and (c) the mean daily rainfall intensity for wet days defined as the regional average rainfall for all days with rainfall > 1 mm.

[24] For southern Sonora, Mexico, wet spells are defined as the mean number of consecutive days with mean regional precipitation ≥1 mm.

[25] Daily rainfall intensity during the monsoon is defined as the regional average rainfall for all days with rainfall ≥ 1 mm.

[26] The linear trend in this time series is significant at the p=0.01 level.

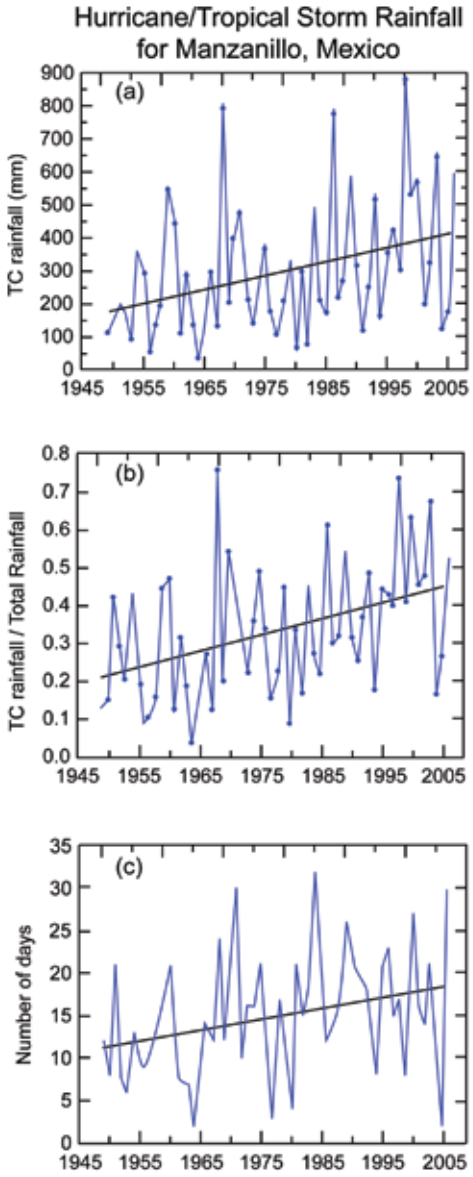


**Figure 2.12** Trends in hurricane/tropical storm rainfall statistics at Manzanillo, Mexico, including: (a) the total warm season rainfall from hurricanes/tropical storms; (b) the ratio of hurricane/tropical storm rainfall to total summer rainfall; and (c) the number of days each summer with a hurricane or tropical storm within 550km of the stations.

the monsoon respond to ENSO, with warm events favoring later starts to the monsoon and shorter length wet spells (days) with cold events favoring opposite behavior (Englehart and Douglas, 2006).

### 2.2.2.5 Tropical Storm Rainfall in Western Mexico

Across southern Baja California and along the southwest coast of Mexico, 30% to 50% of warm season rainfall (May to November) is attributed to tropical cyclones (Figure 2.10), and in years heavily affected by tropical cyclones (upper 95th percentile), 50% to 100% of the summer rainfall comes from tropical cyclones. In this region of Mexico, there is a long-term, upward trend in tropical cyclone-derived rainfall at both Manzanillo (41.8 mm/decade; Figure 2.12a) and Cabo San Lucas (20.5 mm/decade)[27]. This upward trend in tropical cyclone rainfall has led to an increase in the importance of tropical cyclone rainfall in the total warm season rainfall for southwest Mexico (Figure 2.12b), and this has resulted in a higher ratio of tropical cyclone rainfall to total warm season rainfall. Since these two stations are separated by more than 700 km, these significant trends in tropical cyclone rainfall imply large scale shifts in the summer climate of Mexico.

This recent shift in emphasis on tropical cyclone warm season rainfall in western Mexico has strong repercussions as rainfall becomes less reliable from the monsoon and becomes more dependent on heavy rainfall events associated with passing tropical cyclones. Based on the large scale and heavy rainfall characteristics associated with tropical cyclones, reservoirs in the mountainous regions of western Mexico are often recharged by strong tropical cyclone events which therefore have benefits for Mexico despite any attendant damage due to high winds or flooding.

This trend in tropical cyclone-derived rainfall is consistent with a long term analysis of near-shore tropical storm tracks along the west coast of Mexico (storms passing within 5° of the coast) which indicates an upward trend in the number of near-shore storms over the past 50 years (Figure 2.12c, see Englehart *et al.*, 2008). While the number of tropical cyclones occurring in the entire east Pacific basin is uncertain prior to the advent of satellite tracking in about 1967, it should be noted that the long term data sets for near shore storm activity (within 5° of the coast) are considered to be much more reliable due to coastal observatories and heavy ship traffic to and from the Panama Canal to Pacific ports in Mexico and the United States. The number of near shore storm days (storms less than 550 km from the station) has increased by 1.3 days/decade in Manzanillo and about 0.7days/decade in Cabo San Lucas (1949-2006)[28]. The long term correlation between tropical cyclone days at each station and total tropical cyclone rainfall is $r = 0.61$ for Manzanillo and $r = 0.37$ for Cabo San Lucas, illustrating the strong tie between passing tropical cyclones and the rain that they provide to coastal areas of Mexico.

Interestingly, the correlations between tropical cyclone days and total tropical cyclone rainfall actually drop slightly when based only on the satellite era (1967-2006) ( $r = 0.54$ for Manzanillo and $r = 0.31$ for Cabo San Lucas). The fact that the longer time series has the higher set of correlations shows no reason to suggest problems with near shore tropical cyclone tracking in the pre-satellite era. The lower correlations in the more recent period between tropical cyclone days and total tropical cyclone

[27] The linear trends in tropical cyclone rainfall at these two stations are significant at the p=0.01 and p=0.05 level, respectively.

[28] The linear trends in near shore storm days are significant at the p=0.05 level and p=0.10 level, respectively.

rainfall may be tied to tropical cyclone derived rainfall rising at a faster pace compared to the rise in tropical cyclone days. In other words, tropical cyclones are producing more rain per event than in the earlier 1949-1975 period when SSTs were colder.

#### 2.2.2.6 Tropical Storm Rainfall in the Southeastern United States

Tropical cyclone-derived rainfall along the southeastern coast of the United States on a century time scale has changed insignificantly in summer (when no century-long trends in precipitation was observed) as well as in autumn (when the total precipitation increased by more than 20% since the 1900s; Groisman *et al.*, 2004).

#### 2.2.2.7 Streamflow

The flooding in streams and rivers resulting from precipitation extremes can have devastating impacts. Annual average flooding losses rank behind only those of hurricanes. Assessing whether the observed changes in precipitation extremes has caused similar changes in streamflow extremes is difficult for a variety of reasons. First, the lengths of records of stream gages are generally shorter than neighboring precipitation stations. Second, there are many human influences on streamflow that mask the climatic influences. Foremost among these is the widespread use of dams to control streamflow. Vörösmarty *et al.,* (2004) showed that the influence of dams in the United States increased from minor areal coverage in 1900 to a large majority of the U.S. area in 2000. Therefore, long-term trend studies of climatic influences on streamflow have necessarily been very restricted in their areal coverage. Even on streams without dams, other human effects such as land-use changes and stream channelization may influence the streamflow data.

A series of studies by two research groups (Lins and Slack, 1999, 2005; Groisman *et al.*, 2001, 2004) utilized the same set of streamgages not affected by dams. This set of gages represents streamflow for approximately 20% of the contiguous U.S. area. The initial studies both examined the period 1939-1999. Differences in definitions and methodology resulted in opposite judgments about trends in high streamflow. Lins and Slack (1999, 2005) reported no significant changes in high flow above the 90th percentile. On the other hand, Groisman *et al.* (2001) showed that for the same gauges, period, and territory, there were statistically significant regional average increases in the uppermost fractions of total streamflow. However, these trends became statistically insignificant after Groisman *et al.* (2004) updated the analysis to include the years 2000 through 2003, all of which happened to be dry years over most of the eastern United States. They concluded that "… during the past four dry years the contribution of the upper two 5-percentile classes to annual precipitation remains high or (at least) above the average while the similar contribution to annual streamflow sharply declined. This could be anticipated due to the accumulative character of high flow in large and medium rivers; it builds upon the base flow that remains low during dry years…" All trend estimates are sensitive to the values at the edges of the time series, but for high streamflow, these estimates are also sensitive to the mean values of the flow.

Tropical cyclones rank with flash floods as the most lethal and expensive natural catastrophes.

### 2.2.3 Storm Extremes

#### 2.2.3.1 Tropical Cyclones

##### *2.2.3.1.1 Introduction*

Each year, about 90 tropical cyclones develop over the world's oceans, and some of these make landfall in populous regions, exacting heavy tolls in life and property. The global number has been quite stable since 1970, when global satellite coverage began in earnest, having a standard deviation of 10 and no evidence of any substantial trend (*e.g.,*

Hurricane Katrina is estimated to have caused in excess of $80 billion in damages and killed more than 1,500 people. Hurricane Mitch took more than 11,000 lives in Central America.

Webster *et al.*, 2005). However, there is some evidence for trends in storm intensity and/or duration (*e.g.*, Holland and Webster, 2007 and quoted references for the North Atlantic; Chan, 2000, for the Western North Pacific), and there is substantial variability in tropical cyclone frequency within each of the ocean basins they affect. Regional variability occurs on all resolved time scales, and there is also some evidence of trends in certain measures of tropical cyclone energy, affecting many of these regions and perhaps the globe as well.

There are at least two reasons to be concerned with such variability. The first and most obvious is that tropical cyclones rank with flash floods as the most lethal and expensive natural catastrophes, greatly exceeding other phenomena such as earthquakes. In developed countries, such as the United States, they are enormously costly: Hurricane Katrina is estimated to have caused in excess of $80 billion 2005 dollars in damage and killed more than 1,500 people. Death and injury from tropical cyclones is yet higher in developing nations; for example, Hurricane Mitch of 1998 took more than 11,000 lives in Central America. Any variation or trend in tropical cyclone activity is thus of concern to coastal residents in affected areas, compounding trends related to societal factors such as changing coastal population.

A second, less obvious and more debatable issue is the possible feedback of tropical cyclone activity on the climate system itself. The inner cores of tropical cyclones have the highest specific entropy content of any air at sea level, and for this reason such air penetrates higher into the stratosphere than is the case with other storm systems. Thus tropical cyclones may play a role in injecting water, trace gases, and microscopic airborne particles into the upper troposphere and lower stratosphere, though this idea remains largely unexamined. There is also considerable evidence that tropical cyclones vigorously mix the upper ocean, affecting its circulation and biogeochemistry, perhaps to the point of having a significant effect on the climate system. Since the current generation of coupled climate models greatly underresolves tropical cyclones, such feedbacks are badly underrepresented, if they are represented at all. For these reasons, it is important to quantify, understand, and predict variations in tropical cyclone activity. The following sections review current knowledge of these variations on various time scales.

#### *2.2.3.1.2 Data Issues*

Quantifying tropical cyclone variability is limited, sometimes seriously, by a large suite of problems with the historical record of tropical cyclone activity. In the North Atlantic and eastern North Pacific regions, responsibility for the tropical cyclone database rests with NOAA's National Hurricane Center (NHC), while in other regions, archives of hurricane activity are maintained by several organizations, including the U.S. Joint Typhoon Warning Center (JTWC), the Japan Meteorological Agency (JMA), the Hong Kong Observatory (HKO) and the Australian Bureau of Meteorology (BMRC). The data, known as "best track" data (Jarvinen *et al.*, 1984; Chu *et al.*, 2002), comprise a global historical record of tropical cyclone position and intensity, along with more recent structural information. Initially completed in real time, the best tracks are finalized by teams of forecasters who update the best track data at the end of the hurricane season in each ocean basin using data collected during and after each hurricane's lifetime.

It should first be recognized that the primary motivation for collecting data on tropical cyclones was initially to support real-time forecasts, and this remains the case in many regions today. From the 1970s onward, increasing emphasis has been placed on improving the archive for climate purposes and on extending the record back to include historical systems (*e.g.*, Lourensz, 1981; Neumann, 1993; Landsea *et al.*, 2004). Unfortunately, improvements in measurement and estimation techniques have often been implemented with little or no effort

to calibrate against existing techniques, and with poor documentation where such calibrations were done. Thus the available tropical cyclone data contain an inhomogeneous mix of changes in quality of observing systems, reporting policies, and the methods utilized to analyze the data. As one example, the Dvorak technique – a subjective method that is routinely applied in all ocean basins to estimate tropical cyclone intensity using satellite imagery – was not introduced until the early 1970s and has evolved markedly since then. The technique originally utilized visible satellite imagery and was based on subjective pattern recognition. At that time, intensity estimates could only be made during daylight hours. In the early- to mid 1980s, the Dvorak technique was significantly modified to include digital infrared satellite imagery (which is available 24 hours per day), and has become the *de facto* method for estimating intensity in the absence of aircraft reconnaissance. (See Chapter 4 for suggested measures to improve consistency).

Insufficient efforts in re-examining and quality controlling the tropical cyclone record on a year to year basis, particularly outside the Atlantic and eastern North Pacific regions, have resulted in substantial uncertainties when using best track data to calculate changes over time. Efforts are ongoing to reanalyze the historic best track data, but such a *posteriori* reanalyses are less than optimal because not all of the original data that the best track was based on are readily available.

Compared to earlier periods, tropical cyclonecounts are acceptable for application to long-term trend studies back to about 1945 in the Atlantic and 1970 in the Eastern Pacific (*e.g.,* Holland and Webster, 2007 and references therein), and back to about 1975 for the Western and Southern Pacific basins, thanks to earth-orbiting satellites (*e.g.*, Holland, 1981). Until the launch of MeteoSat-7 in 1998, the Indian Oceans were seen only obliquely, but storm counts may still be expected to be accurate after 1977. In earlier periods, it is more likely that storms could be missed entirely, especially if they did not pass near ships at sea or land masses. For the North Atlantic, it is likely that up to 3 storms per year were missing before 1900, dropping to zero by the early 1960s (Holland and Webster, 2007; Chang and Guo, 2007). Estimates of the duration of storms are considered to be less reliable prior to the 1970s due particularly to a lack of good information on their time of genesis. Since the 1970s, storms were more accurately tracked throughout their lifetimes by geostationary satellites.

Estimates of storm intensity are far less reliable, and this remains true for large portions of the globe even today. Airborne hurricane reconnaissance flight became increasingly routine in the North Atlantic and western North Pacific regions after 1945, but was discontinued in the western North Pacific region in 1987. Some missions are today being conducted under the auspices of the government of Taiwan. However, airborne reconnaissance only samples a small fraction of storms, and then only over a fraction of their lifetimes; moreover, good, quantitative estimates of wind speeds from aircraft did not become available until the late 1950s. Beginning in the mid-1970s, tropical cyclone intensity has been estimated from satellite imagery. Until relatively recently, techniques for doing so were largely subjective, and the known lack of homogeneity in both the data and techniques applied in the post-analyses has resulted in significant skepticism regarding the consistency of the intensity estimates in the data set. This lack of temporal consistency renders the data suspect for identifying trends, particularly in metrics related to intensity.

Recent studies have addressed these known data issues. Kossin *et al.* (2007a) constructed a more homogeneous record of hurricane activity, and found remarkably good agreement in

Compared to earlier periods, tropical cyclone counts are acceptable for application to long-term trend studies back to about 1945 in the Atlantic and 1970 in the Eastern Pacific.

It is likely that hurricane activity, as measured by the Power Dissipation Index, has increased substantially since the 1950s and '60s in association with warmer Atlantic sea surface temperatures.

both variability and trends between their new record and the best track data in the North Atlantic and Eastern Pacific basins during the period 1983–2005. They concluded that the best track maintained by the NHC does not appear to suffer from data quality issues during this period. On the other hand, they were not able to corroborate the presence of upward intensity trends in any of the remaining tropical cyclone-prone ocean basins. This could be due to inaccuracies in the satellite best tracks, or could be due to the training of the Kossin *et al.* technique on North Atlantic data. The results of Kossin *et al.* (2007a) are supported by Wu *et al.* (2006), who considered Western Pacific best track data constructed by other agencies (HKMO and JMA) that construct best track data for the western North Pacific. Harper and Callaghan (2006) report on reanalyzed data from the Southeastern Indian Ocean and showed some biases, but an upward intensity trend remains. These studies underscores the need for improved care in analyzing tropical cyclones and in obtaining better understanding of the climatic controls of tropical cyclone activity beyond SST-based arguments alone.

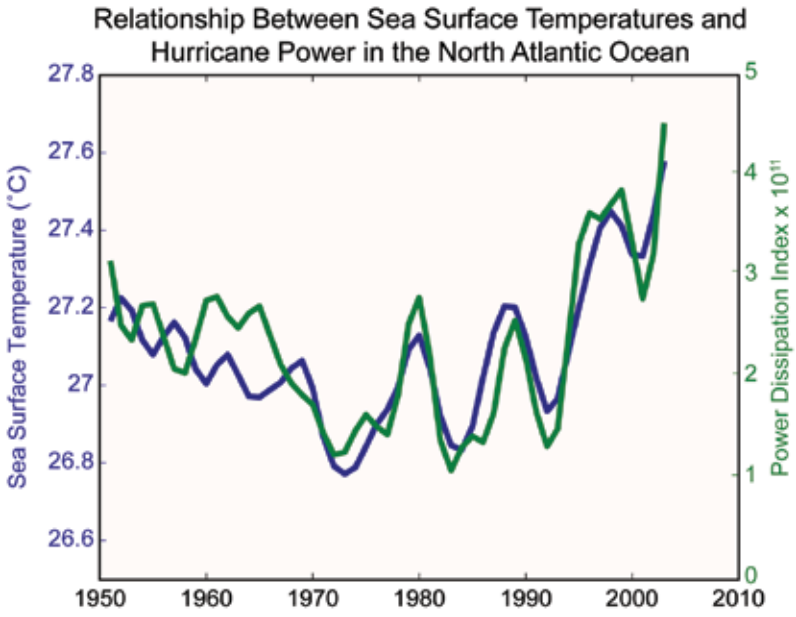


**Figure 2.13** Sea surface temperatures (blue) correlated with the Power Dissipation Index for North Atlantic hurricanes (Emanuel, 2007). Sea Surface Temperature is from the Hadley Centre data set and is for the Main Development Region for tropical cyclones in the Atlantic, defined as 6-18°N, 20-60°W. The time series have been smoothed using a 1-3-4-3-1 filter to reduce the effect of interannual variability and highlight fluctuations on time scales of three years and longer.

The standard tropical cyclone databases do not usually contain information pertaining to the geometric size of tropical cyclones. Exceptions include the Australian region and the enhanced database for the North Atlantic over the last few decades. A measure of size of a tropical cyclone is a crucial complement to estimates of intensity as it relates directly to storm surge and damage area associated with landfalling storms. Such size measures can be inferred from aircraft measurements and surface pressure distributions, and can now be estimated from satellite imagery (*e.g.*, Mueller *et al.*, 2006; Kossin *et al.*, 2007b).

#### *2.2.3.1.3 Low-frequency Variability and Trends of Tropical Cyclone Activity Indices*

"Low frequency" variability is here defined as variations on time scales greater than those associated with ENSO (*i.e.*, more than three to four years). Several papers in recent years have quantified interdecadal variability of tropical cyclones in the Atlantic (Goldenberg *et al.*, 2001; Bell and Chelliah, 2006) and the western North Pacific (Chan and Shi, 1996), attributing most of the variability to natural decade-to-decade variability of regional climates in the Atlantic and Pacific, respectively. In the last few years, however, several papers have attributed both low frequency variability and trends in tropical cyclone activity to changing radiative forcing owing to human-caused particulates (sulfate aerosols) and greenhouse gases.

Emanuel (2005a) developed a "Power Dissipation Index" (PDI) of tropical cyclones, defined as the sum of the cubed estimated maximum sustained surface wind speeds at 6-hour intervals accumulated over each Atlantic tropical cyclone from the late 1940s to 2003. Landsea (2005) commented on the quality of data comprising the index, arguing that the PDI from the 1940s to the mid-1960s was likely underestimated due to limited coverage of the basin by aircraft reconnaissance in that era. An updated version of this analysis (Emanuel 2007), shown in Figure 2.13, confirms that there has been a substantial increase in tropical cyclone activity since about 1970, and indicates that the low-frequency Atlantic PDI variations are strongly correlated with low-frequency variations in tropical Atlantic SSTs. PDI, which integrates over time, is relatively insensitive to

random errors in intensity. Taking into account limitations in data coverage from aircraft reconnaissance and other issues, we conclude that it is likely that hurricane activity, as measured by the Power Dissipation Index (PDI), has increased substantially since the 1950s and '60s in association with warmer Atlantic SSTs. The magnitude of this increase depends on the adjustment to the wind speed data from the 1950s and '60s (Landsea 2005; Emanuel 2007). It is very likely that PDI has generally tracked SST variations on decadal time scales in the tropical Atlantic since 1950, and likely that it also generally tracked the general increase of SST. Confidence in these statistics prior to the late 1940s is low, due mainly to the decreasing confidence in hurricane duration and intensity observations. While there is a global increase in PDI over the last few decades it is not spatially uniform. For example, the PDI in the eastern Pacific has decreased since the early 1980s in contrast to the increase in the tropical Atlantic and some increasing tendency in the western Pacific. (Kossin *et al.*, 2007a; Emanuel *et al.*, 2008).

The Power Dissipation Index for U.S. landfalling tropical cyclones has not increased since the late 1800s (Landsea 2005). Pielke (2005) noted that there are no evident trends in observed damage in the North Atlantic region, after accounting for population increases and coastal development. However, Emanuel (2005b) notes that a PDI series such as Landsea's (2005), based on only U.S. landfalling data, contains only about 1 percent of the data that Emanuel's (2005a) basin-wide PDI contains, which is based on all storms over their entire lifetimes. Thus a trend in basin-wide PDI may not be detectable in U.S. landfalling PDI since the former index has a factor of 10 advantage in detecting a signal in a variable record (the signal-to-noise ratio).

Figure 2.14 (from Holland and Webster, 2007) indicates that there has been no distinct trend in the mean intensity of all Atlantic storms, hurricanes, and major hurricanes. A distinct increase in the most intense storms occurred around the time of onset of aircraft reconnaissance, but this is considered to be largely due to better observing methods. Holland and Webster also found that the overall proportion of hurricanes in the North Atlantic has remained remarkably constant during the 20th century at around 50%, and there has been a marked oscillation in major hurricane proportions, which has no observable trend. Webster *et al.* (2005) reported that the number of category 4 and 5 hurricanes has almost doubled globally over the past three decades. The recent reanalysis of satellite data beginning in the early 1980s by Kossin *et al.* (2007a) support these results in the Atlantic, although the results in the remaining basins were not corroborated.

The recent Emanuel and Webster *et al.* studies have generated much debate in the hurricane research community, particularly with regard to homogeneity of the tropical cyclone data over time and the required adjustments (*e.g.,* Landsea 2005; Knaff and Sampson, 2006; Chan, 2006; Hoyos *et al.,* 2006; Landsea *et al.,* 2006; Sriver and Huber, 2006; Klotzbach, 2006; Elsner *et al.*, 2006; Maue and Hart, 2007; Manning and Hart,2007; Holland and Webster, 2007; Landsea, 2007; Mann *et al.,* 2007; Holland, 2007). Several of these studies argue that data problems preclude determination of significant trends in various tropical cyclone measures, while others provide further evidence in support of reported trends. In some cases, differences between existing historical data sets maintained by different nations can yield strongly contrasting results (*e.g.*, Kamahori *et al.,* 2006).

There is evidence that Atlantic tropical cyclone formation regions have undergone systematic long-term shifts to more eastward developments. These shifts affect track and duration, which subsequently affect intensity.

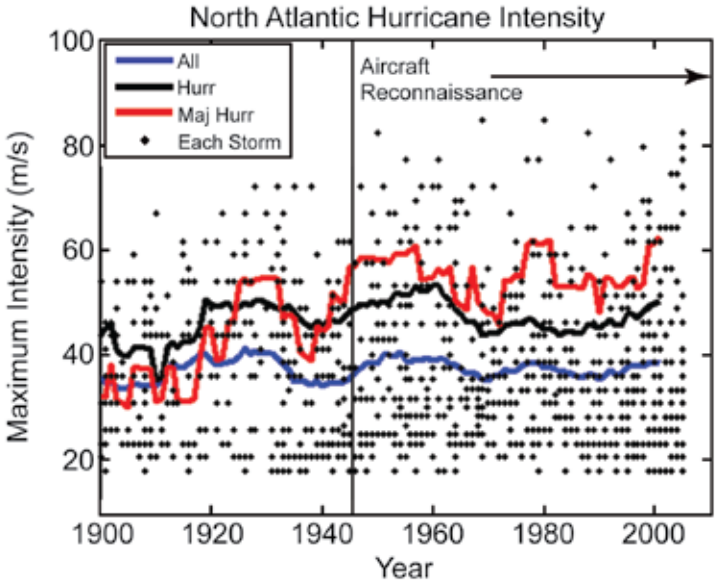


**Figure 2.14** Century changes in the intensity of North Atlantic tropical cyclones, hurricanes, and major hurricanes. Also shown are all individual tropical cyclone intensities. (From Holland and Webster, 2007).

Several studies have examined past regional variability in tropical cyclone tracks (Wu *et al.,* 2005; Xie *et al.,* 2005; Vimont and Kossin, 2007; Kossin and Vimont, 2007). Thus far, no clear long-term trends in tracks have been reported, but there is evidence that Atlantic tropical cyclone formation regions have undergone systematic long-term shifts to more eastward developments (Holland, 2007). These shifts affect track and duration, which subsequently affects intensity. The modulation of the Atlantic tropical cyclone genesis region occurs through systematic changes of the regional SST and circulation patterns. Thus SST affects intensity not just through thermodynamic pathways that are local to the storms, but also through changes in basinwide circulation patterns (Kossin and Vimont, 2007).

Atlantic tropical cyclone counts closely track low-frequency variations in tropical Atlantic sea surface temperatures, including a long-term increase since the late 1800s and early 1900s.

In summary, we conclude that Atlantic tropical storm and hurricane destructive potential as measured by the Power Dissipation Index (which combines storm intensity, duration, and frequency) has increased. This increase is substantial since about 1970, and is likely substantial since the 1950s and '60s, in association with warming Atlantic sea surface temperatures.

#### *2.2.3.1.4 Low-frequency Variability and Trends of Tropical Cyclone Numbers*

Mann and Emanuel (2006) reported that Atlantic tropical cyclone counts closely track low-frequency variations in tropical Atlantic SSTs, including a long-term increase since the late 1800s and early 1900s (see also Figure 2.15 from Holland and Webster, 2007). There is currently debate on the relative roles of internal climate variability (*e.g.*, Goldenberg *et al.,* 2001) versus radiative forcing, including greenhouse gases, and sulfate aerosols (Mann and Emanuel, 2006; Santer *et al.,* 2006) in producing the multi-decadal cooling of the tropical North Atlantic. This SST variation is correlated with reduced hurricane activity during the 1970s and '80s relative to the 1950s and '60s or to the period since 1995 (see also Zhang *et al.,* 2007).

On a century time scale, time series of tropical cyclone frequency in the Atlantic (Figure 2.15) show substantial interannual variability and a marked increase (of over 100%) since about 1900. This increase occurred in two sharp jumps of around 50%, one in the 1930s and another that commenced in 1995 and has not yet stabilized. Holland and Webster (2007) have

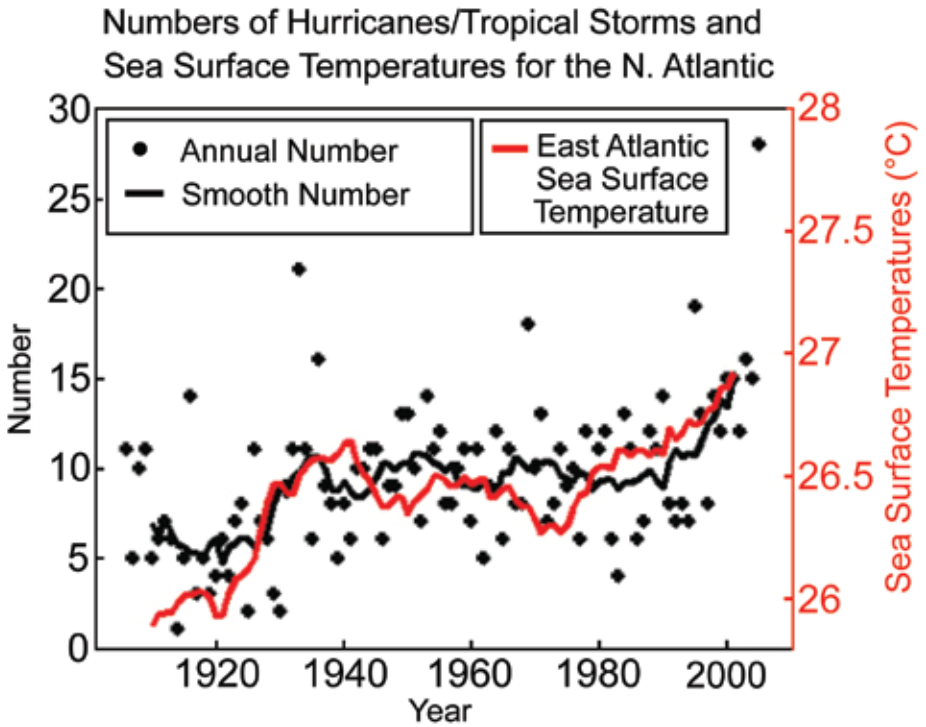


**Figure 2.15** Combined annual numbers of hurricanes and tropical storms for the North Atlantic (black dots), together with a 9-year running mean filter (black line) and the 9-year smoothed sea surface temperature in the eastern North Atlantic (red line). Adapted from Holland and Webster (2007).

suggested that these sharp jumps are transition periods between relatively stable climatic periods of tropical cyclone frequency (Figure 2.15). Figure 2.15 uses unadjusted storm data—an issue which will be addressed further below.

For tropical cyclone frequency, the finding that the largest recorded increases over the past century have been in the eastern North Atlantic (*e.g.*, see recent analysis in Vecchi and Knutson, 2008; Holland, 2007), which historically has been the least well observed, has led to questions of whether this may be due to data issues (Landsea *et al.*, 2004; Landsea, 2007). The major observing system change points over the past century have been:

- The implementation of routine aircraft reconnaissance in 1944-45;
- The use of satellite observations and related analysis procedures from the late 1960s onwards; and
- A change in analysis practice by the National Hurricane Center from 1970 to include more mid-latitude systems.

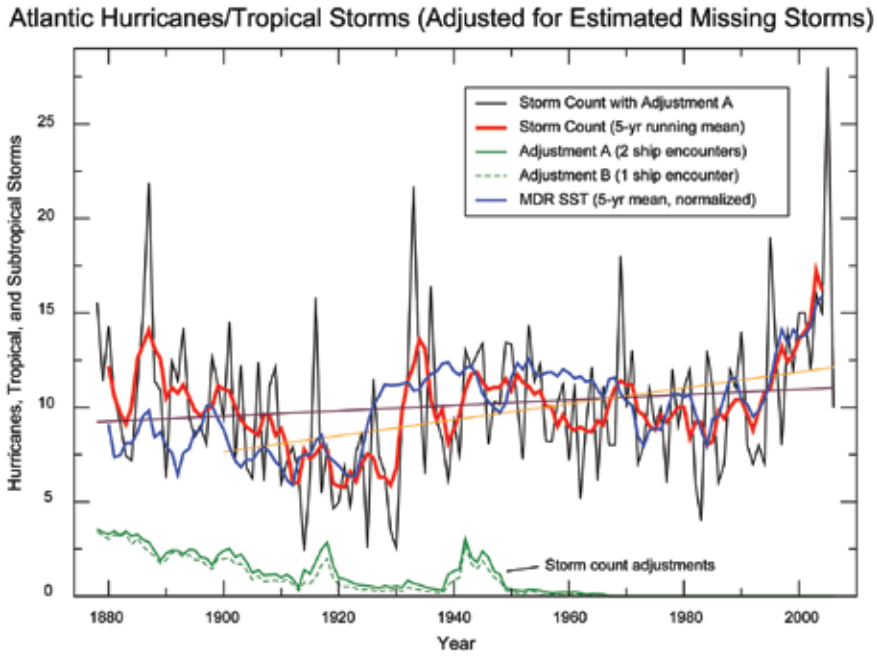


**Figure 2.16** Atlantic hurricanes and tropical storms for 1878-2006, using the adjustment method for missing storms described in the text. Black curve is the adjusted annual storm count, red is the 5-year running mean, and solid blue curve is a normalized (same mean and variance) 5-year running mean sea surface temperature index for the Main Development Region of the tropical Atlantic (HadISST, 80-20°W, 10-20°N; Aug.-Oct.). Green curve shows the adjustment that has been added for missing storms to obtain the black curve, assuming two simulated ship-storm "encounters" are required for a modern-day storm to be "detected" by historical ship traffic for a given year. Straight lines are least squares trend lines for the adjusted storm counts. (Adapted from Vecchi and Knutson, 2008).

In addition, there have been steady improvements in techniques and instrumentation, which may also introduce some spurious trends.

Landsea (2007) has used the fraction of tropical cyclones striking land in the satellite and pre-satellite era to estimate the number of missing tropical cyclones in the pre-satellite era (1900 to 1965) to be about 3.2 per year. He argued that since about 2002, an additional one tropical cyclone per year is being detected due to improved measurement tools and methods. His first adjustment (2.2 per year) assumes that the fraction of all tropical cyclones that strike land in the real world has been relatively constant over time, which has been disputed by Holland (2007). Holland also shows that the smaller fraction of tropical cyclones that made landfall during the past fifty years (1956-2005) compared to the previous fifty years (1906-1955) is related to changes in the main formation location regions, with a decrease in western Caribbean and Gulf of Mexico developments and an increase in the eastern Atlantic.

Alternative approaches to estimating the earlier data deficiencies have been used by Chang and Guo (2007), Vecchi and Knutson (2008), and Mann *et al.* (2007). The first two studies use historical ship tracks from the pre-satellite era, combined with storm track information from the satellite era, to infer an estimated adjustment for missing storms in the pre-satellite era (assumed as all years prior to 1965). Mann *et al.* used statistical climate relationships to estimate potential errors. Vecchi and Knutson found 2 to 3 storms per year were missing prior to 1900, decreasing to near zero by 1960. Chang and Guo found 1.2 storms missing around 1910, also decreasing to near zero by 1960. Mann *et al.* estimated a more modest undercount bias of 1 per year prior to 1970. The adjusted time series by Vecchi and Knutson (Figure 2.16) suggest a statistically significant (p=0.002 or less) positive linear trend in adjusted storm counts of 55% per century since 1900. However, beginning the trend from 1878, the trend through 2006 is

There has been an increase in both overall storm frequency and the proportion of major hurricanes since 1995. Taken together, these result in a very sharp increase in major hurricane numbers, which can be associated with changes of sea surface temperature.

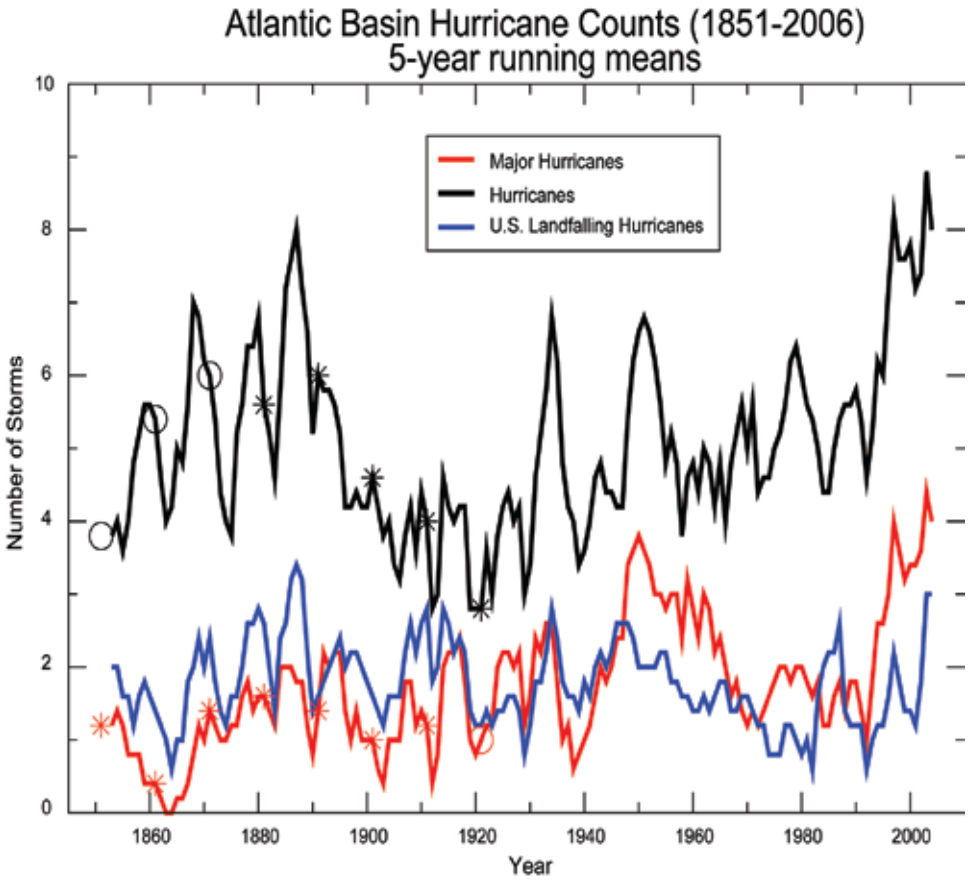


**Figure 2.17** Counts of total North Atlantic basin hurricanes (black), major hurricanes (red), and U.S. landfalling hurricanes (blue) based on annual data from 1851 to 2006 and smoothed (using a 5-year running mean). Asterisks on the time series indicate years where trends beginning in that year and extending through 2005 are statistically significant (p=0.05) based on annual data; circles indicate non-significant trend results (data obtained from NOAA's Oceanographic and Meteorological Laboratory: http://www.aoml.noaa.gov/hrd/hurdat/ushurrlist18512005-gt.txt).

smaller (+15% per century) and not statistically significant at the p=0.05 level (p-value of about 0.2)[29]. It is notable that the degree of increase over the past century depends on the analysis methodology. When using a linear trend, as above, the increase from 1900 to 2005 is around 55% in the adjusted storm counts. However, using the essentially non-linear approach by Holland and Webster (2007) of separate climatic regimes, the increase in adjusted storm counts from the 1900-1920 regime to the 1995-2006 regime is 85%. The trend from 1900 begins near a local minimum in the time series and ends with the recent high activity, perhaps exaggerating the significance of the trend due to multidecadal variability. On the other hand, high levels of activity during the late 1800s, which lead to the insignificant trend result, are indirectly inferred in large part from lack of ship track data, and the uncertainty in the late 1800s storm counts is greater than that during the 1900s.

Hurricane frequency closely follows the total tropical cyclone variability, with a stable 50% of all cyclones developing to hurricane strength over much of the past century (Holland and Webster, 2007). However, there has been a concomitant increase in both overall storm frequency and the proportion of major hurricanes since 1995. Taken together, these result in a very sharp increase in major hurricane numbers, which can be associated with changes of SST (Holland and Webster, 2007; Webster *et al.,* 2005). The PDI trend reported by Emanuel (2007) is largely due to this increase in major hurricane numbers.

Atlantic basin total hurricane counts, major hurricane counts, and U.S. landfalling hurricane counts as recorded in the HURDAT data base for the period 1851-2006 are shown in Figure 2.17. These have not been adjusted for missing storms, as there was likely less of a tendency to miss both hurricanes and major hurricanes in earlier years compared to tropical storms, largely because of their intensity and damage potential. However, even though intense storms were less likely than weaker systems to be missed entirely, lack of satellite coverage and other data issues imply that it would have been much more difficult to measure their maximum intensity accurately, leading to a potential undercount in the hurricane and major hurricane numbers. Using the unadjusted data, hurricane counts ending in 2005 and beginning in 1881 through 1921 increased and are statistically significant (p=0.05), whereas trends beginning in 1851 through 1871 are not statistically significant, owing to the high counts reported from 1851 to 1871. For major hurricanes, trends to 2005 beginning in 1851 through 1911 show

[29] Details of the statistical analysis are given in the Appendix, Example 5.

an increase and are statistically significant, whereas the trend beginning from 1921 also shows an increase but is not statistically significant[30]. The significant increase since 1900 in hurricane and major hurricane counts is supported by the significant upward trends in tropical storm counts since 1900 and the observation that hurricane and major hurricane counts as a proportion of total tropical cyclone counts are relatively constant over the long term (Holland and Webster, 2007). Regarding the trends from the 1800s, the lack of significant trend in hurricane counts from earlier periods is qualitatively consistent with the lack of significant trend in adjusted tropical storm counts from 1878 (Figure 2.16). For major hurricanes, the counts from the late 1800s, and thus the significant positive trends from that period, are considered less reliable, as the proportion of storms that reached major hurricane intensity, though relatively constant over the long-term in the 20th century, decreases strongly prior to the early 1900s, suggestive of strong data inhomogeneities. There is no evidence for a significant trend in U.S. landfalling hurricane frequency.

Regional storm track reconstructions for the basin (Vecchi and Knutson, 2008; Holland and Webster, 2007) indicate a decrease in tropical storm occurrence in the western part of the basin, consistent with the minimal change or slight decrease in U.S. landfalling tropical storm or hurricane counts. These analyses further suggest that—after adjustment for missing storms—an increase in basin-wide Atlantic tropical cyclone occurrence has occurred since 1900, with increases mainly in the central and eastern parts of the basin (also consistent with Chang and Guo, 2007). From a climate variability perspective, Kossin and Vimont (2007) have argued that the Atlantic Meridional Mode is correlated to a systematic eastward extension of the genesis region in the Atlantic. Kimberlain and Elsner (1998) and Holland and Webster (2007) have shown that the increasing frequency over the past 30 years is associated with a changeover to equatorial storm developments, and particularly to developments in the eastern equatorial region. Over the past century, the relative contributions of data fidelity issues (Landsea, 2007) versus real climatic modulation (Landsea *et al.*, 1999; Kimberlain and Elsner, 1998; Kossin and Vimont, 2007; Holland and Webster, 2007) to the apparent long-term increase in eastern Atlantic tropical storm activity is presently an open question.

In summary, we conclude that there have been fluctuations in the number of tropical storms and hurricanes from decade to decade, and data uncertainty is larger in the early part of the record compared to the satellite era beginning in 1965. Even taking these factors into account, it is likely that the annual numbers of tropical storms, hurricanes, and major hurricanes in the North Atlantic have increased over the past 100 years, a time in which Atlantic sea surface temperatures also increased. The evidence is less compelling for significant trends beginning in the late 1800s. The existing data for hurricane counts and one adjusted record of tropical storm counts both indicate no significant linear trends beginning from the mid- to late 1800s through 2005. In general, there is increasing uncertainty in the data as one proceeds back in time. There is no evidence for a long-term increase in North American mainland land-falling hurricanes.

It is likely that the annual numbers of tropical storms, hurricanes, and major hurricanes in the North Atlantic have increased over the past 100 years, a time in which Atlantic sea surface temperatures also increased.

#### *2.2.3.1.5 Paleoclimate Proxy Studies of Past Tropical Cyclone Activity*

Paleotempestology is an emerging field of science that attempts to reconstruct past tropical cyclone activity using geological proxy evidence or historical documents. This work attempts to expand knowledge about hurricane occurrence back in time beyond the limits

[30] Further details of the statistical analysis are given in Appendix A, Example 6.

of conventional instrumental records, which cover roughly the last 150 years. A broader goal of paleotempestology is to help researchers explore physically based linkages between prehistoric tropical cyclone activity and other aspects of past climate.

Among the geologically-based proxies, overwash sand layers deposited in coastal lakes and marshes have proven to be quite useful (Liu and Fearn, 1993, 2000; Liu, 2004; Donnelly and Webb, 2004). Similar methods have been used to produce proxy records of hurricane strikes from back-barrier marshes in Rhode Island and New Jersey extending back about 700 years (Donnelly *et al.*, 2001a, 2001b; Donnelly *et al.*, 2004; Donnelly and Webb, 2004), and more recently in the Caribbean (Donnelly, 2005). Stable isotope signals in tree rings (Miller *et al.*, 2006), cave deposits (Frappier *et al.*, 2007) and coral reef materials are also being actively explored for their utility in providing paleoclimate information on tropical cyclone activity. Historical documents apart from traditional weather service records (newspapers, plantation diaries, Spanish and British historical archives, *etc.*) can also be used to reconstruct some aspects of past tropical cyclone activity (Ludlum, 1963; Millás, 1968; Fernández-Partagás and Diaz, 1996; Chenoweth, 2003; Mock, 2004; García Herrera *et al.*, 2004; 2005; Liu *et al.*, 2001; Louie and Liu, 2003, 2004).

Combined with non-tropical storms, rising sea level extends the zone of impact from storm surge and waves farther inland, and will likely result in increasingly greater coastal erosion and damage.

Donnelly and Woodruff's (2007) proxy reconstruction of the past 5,000 years of intense hurricane activity in the western North Atlantic suggests that hurricane variability has been strongly modulated by El Niño during this time, and that the past 250 years has been relatively active in the context of the past 5,000 years. Nyberg *et al.* (2007) suggest that major hurricane activity in the Atlantic was anomalously low in the 1970s and 1980s relative to the past 270 years. As with Donnelly and Woodruff, their proxy measures were located in the western part of the basin (near Puerto Rico), and in their study, hurricane activity was inferred indirectly through statistical associations with proxies for vertical wind shear and SSTs.

### 2.2.3.2 Strong Extratropical Cyclones Overview

Extra-tropical cyclone (ETC)[31] is a generic term for any non-tropical, large-scale low pressure storm system that develops along a boundary between warm and cold air masses. These types of cyclonic[32] disturbances are the dominant weather phenomenon occurring in the mid- and high latitudes during the cold season because they are typically large and often have associated severe weather. The mid-latitude North Pacific and North Atlantic basins, between approximately 30°N-60°N, are regions where large-numbers of ETCs develop and propagate across the ocean basins each year. Over land or near populous coastlines, strong or extreme ETC events generate some of the most devastating impacts associated with extreme weather and climate, and have the potential to affect large areas and dense population centers. A notable example was the blizzard of 12-14 March 1993 along the East Coast of the United States that is often referred to as the "super-storm" or "storm of the century"[33] (*e.g.*, Kocin *et al.*, 1995). Over the ocean, strong ETCs generate high waves that can cause extensive coastal erosion when combined with storm surge as they reach the shore, resulting in significant economic impact. Rising sea level extends the zone of impact

[31] The fundamental difference between the characteristics of extra-tropical and tropical cyclones is that ETCs have a cold core and their energy is derived from baroclinic instability, while tropical cyclones have a warm core and derive their energy from barotropic instability (Holton, 1979).

[32] A term applied to systems rotating in the counter-clockwise direction in the Northern Hemisphere.

[33] The phrase "Storm of the Century" is also frequently used to refer to the 1991 Halloween ETC along the Northeast US coast, immortalized in the book and-movie *The Perfect Storm* (Junger, 1997).

from storm surge and waves farther inland, and will likely result in increasingly greater coastal erosion and damage from storms of equal intensity.

Studies of changes in strong ETCs and associated frontal systems have focused on locations where ETCs form, and the resulting storm tracks, frequencies, and intensities[34]. The primary constraint on these studies has been the limited period of record available that has the best observation coverage for analysis and verification of results, with most research focused on the latter half of the 20th century. Model reanalysis data is used in the majority of studies, either NCEP-NCAR (Kalnay *et al.*, 1996) or ERA-40 (Upalla *et al.*, 2005) data sets, although prior to 1965, data quality has been shown to be less reliable.

It is important to stress that any observed changes in ETC storm tracks, frequencies, or intensities are highly dependent on broad-scale atmospheric modes of variability, and the noise associated with this variability is large in relation to any observed linear trend. Therefore, detection and attribution of long-term (decade-to-century-scale) changes in ETC activity is extremely difficult, especially when considering the relatively short length of most observational records.

#### *2.2.3.2.1 Variability of Extra-Tropical Cyclone Activity*

Inter-annual and inter-decadal variability of ETCs is primarily driven by the location and other characteristics associated with the Polar jet stream. The mean location of the Polar jet stream is often referred to as the "storm track." The large-scale circulation is governed by the equator-to-pole temperature gradient, which is strongly modulated by SSTs over the oceans. The magnitude of the equator-to-pole temperature gradient is an important factor in determining the intensity of storms: the smaller (larger) the gradient in temperature, the smaller (larger) the potential energy available for extra-tropical cyclone formation. The observed intensity of ETCs at the surface is related to the amplitude of the large-scale circulation pattern, with high-amplitude, negatively tilted troughs favoring stronger development of ETCs at the surface (Sanders and Gyakum, 1980).

From a seasonal perspective, the strongest ETCs are temporally out of phase in the Pacific and Atlantic basins, since the baroclinic wave energy climatologically reaches a peak in late fall in the North Pacific and in January in the North Atlantic (Nakamura, 1992; Eichler and Higgins, 2006). While it remains unclear what the physical basis is for the offset in peak storm activity between the two basins, Nakamura (1992) showed statistically that when the Pacific jet exceeds 45 m per second, there is a suppression of baroclinic wave energy, even though the low-level regional baroclinicity and strength of the Pacific jet are at a maximum. (This effect is not evident in the Atlantic basin, since the peak strength of the jet across the basin rarely exceeds 45 m per second). Despite the observed seasonal difference in the peak of ETC activity, Chang and Fu (2002) found a strong positive correlation between the Pacific and Atlantic storm tracks using monthly mean reanalysis data covering 51 winters (1949 to 1999). They found the correlations between the two basins remained positive and robust over individual months during winter (DJF) or over the entire season (Chang and Fu, 2002).

It has been widely documented that the track position, intensity, and frequency of ETCs is strongly modulated on inter-annual time-scales by different modes of variability, such as the El Niño/Southern Oscillation (ENSO) phenomenon (Gershunov and Barnett, 1998; An *et al.*, 2007). In a recent study, Eichler and Higgins (2006) used both NCEP-NCAR and ERA-40 reanalysis data to diagnose the behavior of ETC activity during different ENSO phases. Their results showed that during El Niño events, there is an equatorward shift in storm tracks in the North Pacific basin, as well as an increase of storm track activity along the United States East Coast. However, they found significant variability related to the magnitude of the El Niño event. During strong El Niños, ETC frequencies peak over the North Pacific and along the eastern United States, from the southeast coast to the Maritime Provinces of Canada (Eichler and Higgins, 2006), with a secondary track across the Midwest from the

During El Niño events, there is an equatorward shift in storm tracks in the North Pacific basin, as well as an increase of storm track activity along the United States East Coast.

[34] These studies use *in situ* observations (both surface and upper-air), reanalysis fields, and Atmospheric-Ocean Global Climate Model (GCM) hind casts.

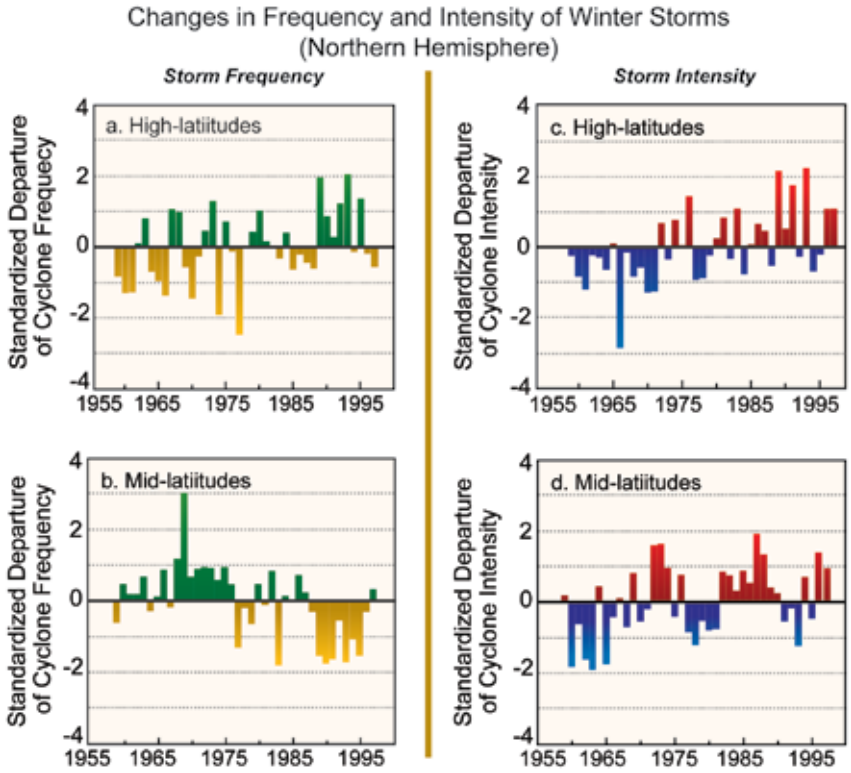


**Figure 2.18** Changes from average (1959-1997) in the number of winter (Nov-Mar) storms each year in the Northern Hemisphere for: (a) high latitudes (60°-90°N), and (b) mid-latitudes (30°-60°N), and the change from average of winter storm intensity in the Northern Hemisphere each year for (c) high latitudes (60°-90°N), and (d) mid-latitudes (30°-60°N). (Adapted from McCabe *et al.*, 2001).

lee of the Rocky Mountains to the Great Lakes. During weak to moderate El Niños, the storm tracks are similar to the strong El Niños, except there is a slight increase in the number of ETCs over the northern Plains, and the frequency of ETC activity decreases over the mid-Atlantic region. Similar to other previous studies (*e. g.* Hirsch *et al.*, 2001; Noel and Changnon, 1998), an inverse relationship typically exists during La Niñas; as the strength of La Niña increases, the frequency maxima of East Coast storms shifts poleward, the North Pacific storm track extends eastward toward the Pacific Northwest, and the frequency of cyclones increases across the Great Lakes region (Eichler and Higgins, (2006).

In addition to ENSO, studies have shown that the Arctic Oscillation (AO) can strongly influence the position of storm tracks and the intensity of ETCs. Previous studies have shown that during positive AO conditions, Northern Hemisphere cyclone activity shifts poleward (Serreze *et al.*, 1997; Clark *et al.*, 1999). Inversely, during negative AO conditions, the polar vortex is weaker and cyclone activity shifts southward. Since the North Atlantic Oscillation (NAO) represents the primary component of the AO, it has a similar effect on storm track position, especially over the eastern North Atlantic basin (McCabe *et al.*, 2001).

### *2.2.3.2.2 Changes in Storm Tracks and Extra-Tropical Cyclone Characteristics*

Many studies have documented changes in storm track activity. Specifically, a significant northward shift of the storm track in both the Pacific and Atlantic ocean basins has been verified by a number of recent studies that have shown a decrease in ETC frequency in mid-latitudes, and a corresponding increase in ETC activity in high latitudes (Wang *et al.*, 2006a; Simmonds and Keay, 2002; Paciorek *et al.*, 2002; Graham and Diaz, 2001; Geng and Sugi, 2001; McCabe *et al.*, 2001; Key and Chan, 1999; Serreze *et al.*, 1997). Several of these studies have examined changes in storm tracks over the entire Northern Hemisphere (McCabe *et al.*, 2001; Paciorek *et al.*, 2002; Key and Chan, 1999), while several others have focused on the storm track changes over the Pacific (Graham and Diaz, 2001) and Atlantic basins (Geng and Sugi, 2001), or both (Wang and Swail, 2001). Most of these studies focused on changes in frequency and intensity observed during winter (Dec., Jan., Feb.) or the entire cold season (Oct.-Mar.). However, for spring, summer, and autumn, Key and Chan (1999) found opposite trends in 1000-hPa and 500-hPa cyclone frequencies for both the mid- and high latitudes of the Northern Hemisphere. The standardized annual departures[35] of ETC frequency for the entire Northern Hemisphere over the period 1959-1997 (Figure 2.18a,b; McCabe *et al.*, 2001) shows that cyclone frequency has decreased for the mid-latitudes (30°-60°N) and increased for the high latitudes (60°-90°N).

A significant northward shift of the storm track in both the Pacific and Atlantic ocean basins has been verified by a number of recent studies.

[35] Standardized departures (*z* scores) were computed for each 5° latitudinal band by subtracting the respective 1959-1997 mean from each value and dividing by the respective 1959-1997 standard deviation (McCabe *et al.*, 2001).

For the 55-year period of 1948-2002, a metric called the Cyclone Activity Index (CAI)[36] was developed by Zhang *et al.* (2004) to document the variability of Northern Hemisphere cyclone activity. The CAI has increased in the Arctic Ocean (70°-90°N) during the latter half of the 20th century, while it has decreased in mid-latitudes (30°-60°N) from 1960 to 1993, which is evidence of a poleward shift in the average storm track position. Interestingly, the number and intensity of cyclones entering the Arctic from the mid-latitudes has increased, particularly during summer (Zhang *et al.*, 2004). The increasing activity in the Arctic was more recently verified by Wang *et al.* (2006a), who analyzed ETC counts by applying two separate cyclone detection thresholds to ERA-40 reanalysis of mean sea level pressure data. Their results showed an increase in high latitude storm counts, and a decrease in ETC counts in the mid-latitudes during the latter half of the 20th century.

Northern Hemisphere ETC intensity has increased over the period 1959-1997 across both mid- and high latitudes cyclone intensity (McCabe *et al.*, 2001; Figure 2.18c,d), with the upward trend more significant for the high latitudes (0.01 level) than for the mid-latitudes (0.10 level). From an ocean basin perspective, the observed increase in intense ETCs appears to be more robust across the Pacific than the Atlantic. Using reanalysis data covering the period 1949-1999, Paciorek *et al.* (2002) found that extreme wind speeds have increased significantly in both basins (Figure 2.19a,d). Their results also showed that the observed upward trend in the frequency of intense cyclones has been more pronounced in the Pacific basin (Figure 2.19c), although the inter-annual variability is much less in the Atlantic (Figure 2.19f). Surprisingly, they found that the overall counts of ETCs showed either no long-term change, or a decrease in the total number of cyclones (Figure 2.19b,e). However, this may be a result of the large latitudinal domain used in their study (20°-70°N), which included parts of the tropics, sub-tropics, mid- and high latitudes.

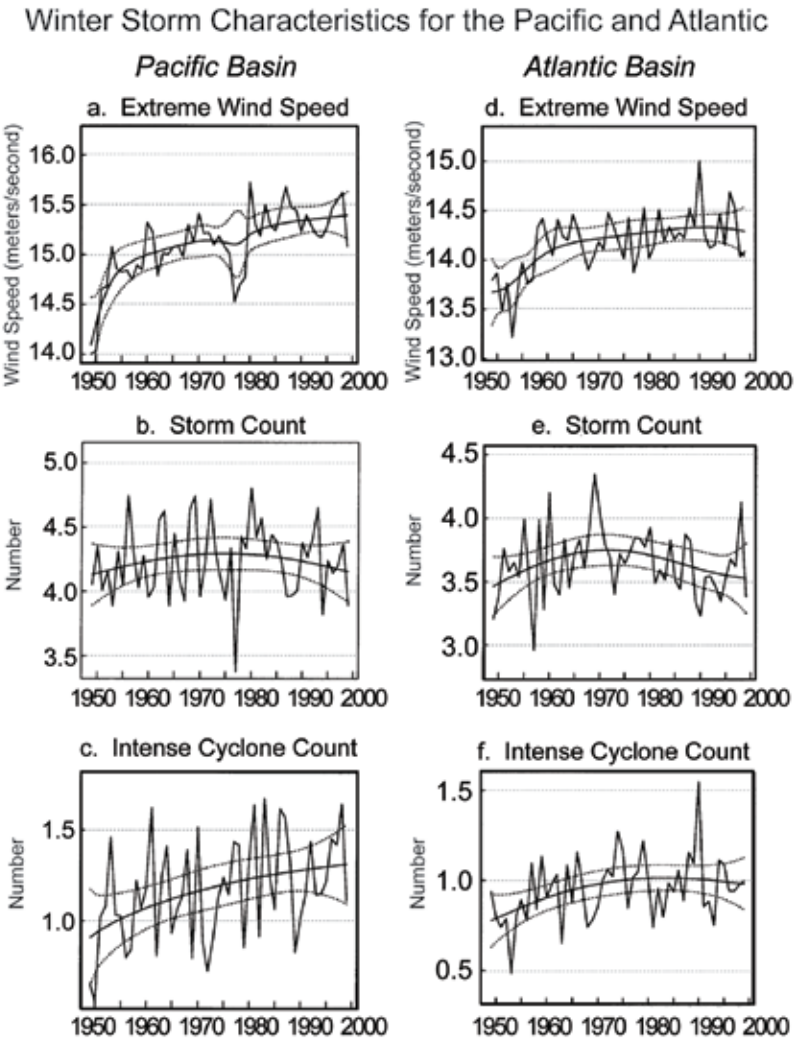


**Figure 2.19** Extreme wind speed (meters per second), number of winter storms, and number of intense (≤980 hPa) winter storms for the Pacific region (20°-70°N, 130°E-112.5°W; panels a-b-c) and the Atlantic region (20°-70°N, 7.5°E-110°W; panels d-e-f). The thick smooth lines are the trends determined using a Bayesian spline model, and the thin dashed lines denote the 95% confidence intervals. (Adapted from Paciorek *et al.*, 2002).

On a regional scale, ETC activity has increased in frequency, duration, and intensity in the lower Canadian Arctic during 1953-2002, with the most statistically significant trends during winter[37] (p=0.05 level; Wang *et al.*, 2006b). In contrast to the Arctic region, cyclone activity was less frequent and weaker along the southeast and southwest coasts of Canada. Winter cyclone deepening rates (*i.e.*, rates of intensification) have increased in the zone around 60°N, but decreased further south in the Great Lakes area and southern Prairies-British Columbia region

Extreme wind speeds in storms outside the tropics have increased significantly in both the Atlantic and Pacific basins

[36] The CAI integrates information on cyclone intensity, frequency, and duration into a comprehensive index of cyclone activity. The CAI is defined as the sum over all cyclone centers, at a 6-hourly resolution, of the differences between the cyclone central SLP and the climatological monthly mean SLP at corresponding grid points in a particular region during the month (Zhang *et al.*, 2004).

[37] Results based on hourly average sea level pressure data observed at 83 stations.

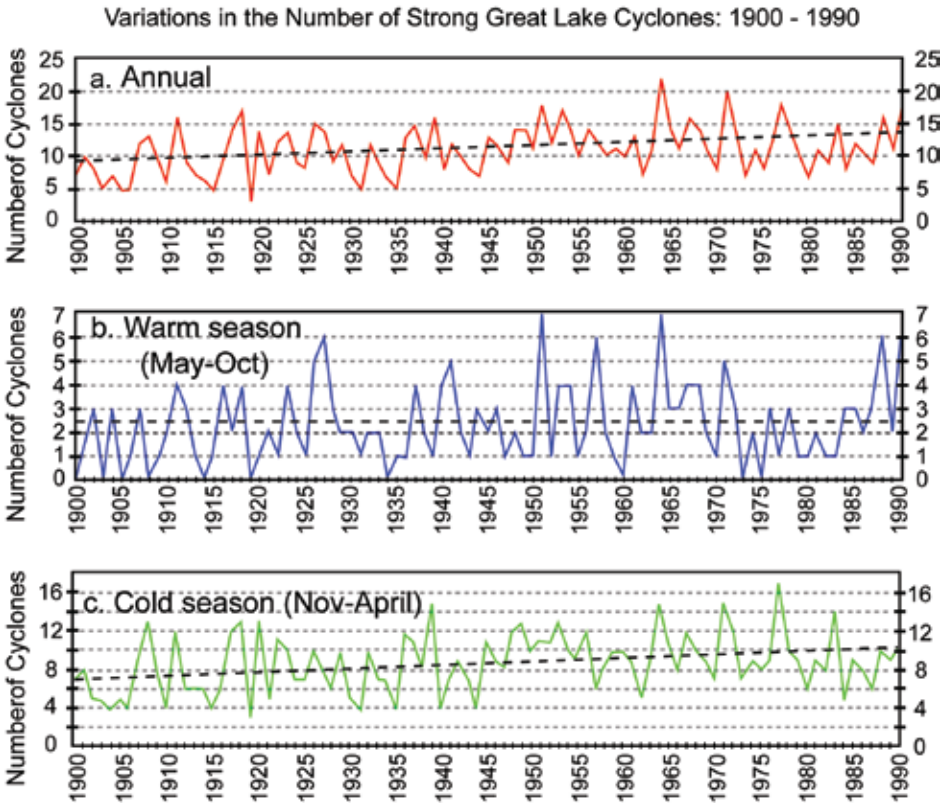


**Figure 2.20** Time series of the number of strong (≤992 hPa) cyclones across the Great Lakes region (40°-50°N, 75°-93°W) over the period 1900-1990 for (a) Annual, (b) Warm season (May-Oct), and (c) Cold season (Nov-Apr). All trends were significant at the 95% level. (Adapted from Angel and Isard, 1998).

Over the period 1900 to 1990, the number of strong storms increased significantly across the Great Lakes, more than doubling for both November and December.

of Canada. This is also indicative of a poleward shift in ETC activity, and corresponding weakening of ETCs in the mid latitudes and an increase in observed intensities in the high latitudes. For the period of 1949-1999, the intensity of Atlantic ETCs increased from the 1960s to the 1990s during the winter season[38] (Harnik and Chang, 2003). Their results showed no significant trend in the Pacific region, but this is a limited finding because of a lack of upper-air (*i.e.*, radiosonde) data over the central North Pacific[39] in the region of the storm track peak (Harnik and Chang, 2003).

There have been very few studies that have analyzed the climatological frequencies and intensities of ETCs across the central United States, specifically in the Great Lakes region (*e.g.*, Lewis, 1987; Harman *et al.*, 1980; Garriott, 1903). Over the period 1900 to 1990, the number of strong cyclones (≤992 mb) increased significantly across the Great Lakes (Angel and Isard, 1998). This increasing trend was evident (at the p=0.05 level) both annually and during the cold season (Figure 2.20). In fact, over the 91-year period analyzed, they found that the number of strong cyclones per year more than doubled during both November and December.

In addition to studies using reanalysis data, which have limited record lengths, other longer-term studies of the variability of *storminess* typically use wave or water level measurements as proxies for storm frequency and intensity. Along the United States West Coast, one of the longest continuous climate-related instrumental time series in existence is the hourly tide gauge record at San Francisco that dates back to 1858. A derived metric called non-tide residuals (NTR)[40], which are related to broad-scale atmospheric circulation patterns across the eastern North Pacific that affect storm track location, provides a measure of *storminess* variability along the California coast (Bromirski *et al.*, 2003). Average monthly variations in NTR, which are associated with the numbers and intensities of all ETCs over the eastern North Pacific, did not change substantially over the period 1858-2000 or over the period covered by most ETC reanalysis studies (1951-2000). However, the highest 2% of extreme winter NTR (Figure 2.21), which are related to the intensity of the most extreme ETCs, had a significant upward trend since approximately 1950, with a pronounced quasi-periodic decadal-scale variability that is relatively consistent over the last 140 years. Changes in storm inten-

[38] Results based on gridded rawinsonde observations covering the Northern Hemisphere.

[39] Besides the few radiosonde sites located on islands (*i.e.,* Midway or the Azores), most upper-air observations over the vast expanses of the North Pacific and Atlantic are from automated pilot reports (pireps) that measure temperature, wind speed, and barometric pressure onboard commercial aircraft traveling at or near jet stream level (between 200-300 hPa).

[40] Non-tide residuals are obtained by first removing the known tidal component from the water level variations using a spectral method; then, variations longer than 30 days and shorter than 2.5 days are removed with a bandpass filter.

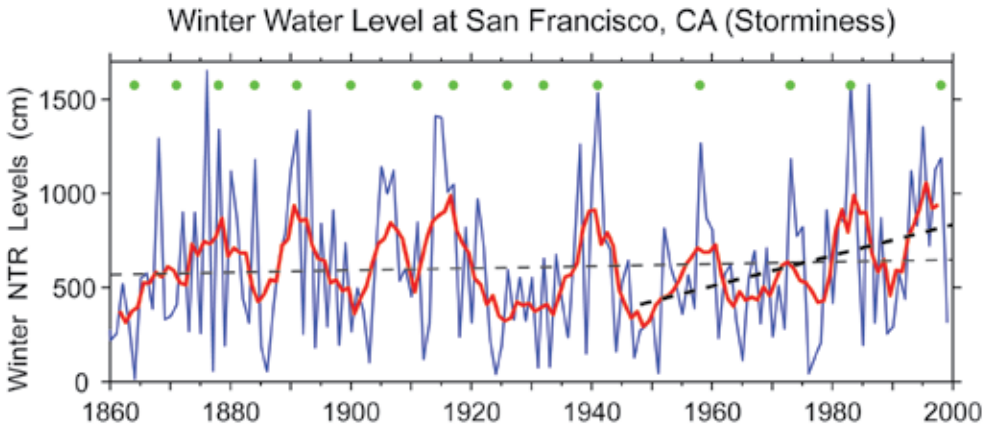


**Figure 2.21** Cumulative extreme Non-Tide Residuals (NTR) water levels exceeding the hourly 98th percentile NTR levels at San Francisco, during winter months (Dec-Mar), with the 5-yr running mean (red line). Least squares trend estimates for the entire winter record (light dashed line; not significant) and since 1948 (bold dashed line; significant at the 97.5% level), the period covered by NCEP reanalysis and ERA-40 data used in most ETC studies. (Adapted from Bromirski *et al.*, 2003).

sity from the mid-1970s to early 1980s are also suggested by substantial pressure decreases at an elevation above sea level of about 3000 m over the eastern North Pacific and North America (Graham, 1994), indicating that the pattern of variability of extreme storm conditions observed at San Francisco (as shown in Figure 2.21) likely extends over much of the North Pacific basin and the United States. The oscillatory pattern of variability is thought to be influenced by teleconnections from the tropics, predominately during ENSO events (Trenberth and Hurrell, 1994), resulting in a deepened Aleutian low shifted to the south and east that causes both ETC intensification and a shift in storm track. It is interesting to note that peaks in the 5-year moving average in Figure 2.21 generally correspond to peaks in extreme rainfall in Figure 2.10, suggesting that the influence of El Niño and broad-scale atmospheric circulation patterns across the Pacific that affect sea level variability along the West Coast are associated with storm systems that affect rainfall variability across the United States.

The amplitude and distribution of ocean wave energy measured by ocean buoys is determined by ETC intensity and track location. Changes in long period (>12 sec), intermediate period, and short period (<6 sec) components in the wave-energy spectra permit inferences regarding the changes over time of the paths of the storms, as well as their intensities and resulting wave energies (Bromirski *et al.*, 2005). Analysis of the combination of observations from several buoys in the eastern North Pacific supports a progressive northward shift of the dominant Pacific storm tracks to the central latitudes (section 2.2.3.3).

#### *2.2.3.2.3 Nor'easters*

Those ETCs that develop and propagate along the East Coast of the United States and southeast Canada are often termed colloquially as *Nor'easters*[41]. In terms of their climatology and any long-term changes associated with this subclass of ETCs, there are only a handful of studies in the scientific literature that have analyzed their climatological frequency and intensity (Jones and Davis 1995), likely due to a lack of any formal objective definition of this important atmospheric phenomenon (Hirsch *et al.*, 2001).

Because waves generated by ETCs are a function of storm size and the duration and area over which high winds persist, changes in significant wave heights can also be used as a proxy for changes in Nor'easters. Using hindcast wave heights and assigning a minimum criterion of open ocean waves greater than 1.6 m in height (a commonly used threshold for storms that caused some degree of beach erosion along the mid-Atlantic coast) to qualify as a nor'easter, the frequency of nor'easters along the Atlantic coast peaked in the 1950s, declined to a minimum in the 1970s, and then increased again to the mid-1980s (Dolan *et al.*, 1988; Davis *et al.*, 1993).

An alternate approach (Hirsch *et al.*, 2001) uses the NCEP-NCAR reanalysis pressure field to determine the direction of movement and wind speed to identify storm systems, and generically names them as East Coast Winter

The pattern of variability of extreme storm conditions observed at San Francisco (as shown in Figure 2.21) likely extends over much of the North Pacific basin and the United States.

[41] According to the *Glossary of Meteorology* (Huschke, 1959), a *nor'easter* is any cyclone forming within 167 km of the East Coast between 30°-40°N and tracking to the north-northeast.

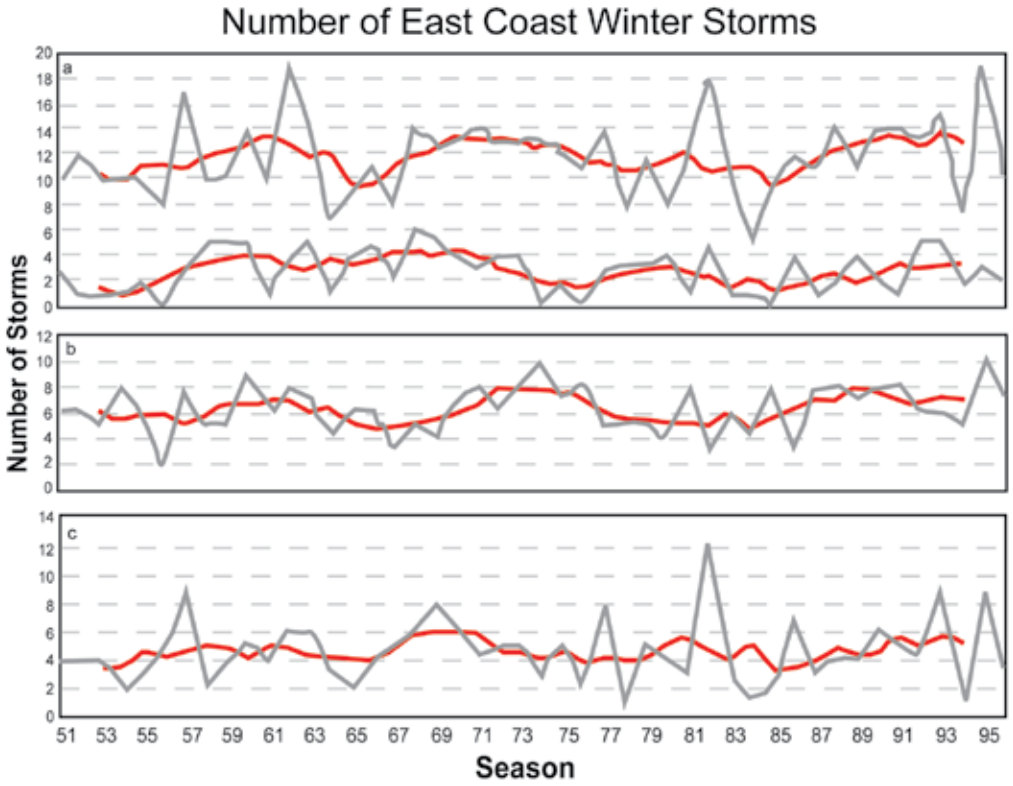


**Figure 2.22** Seasonal totals (gray line) covering the period of 1951-1997 for: (a) all East Coast Winter Storms (ECWS; top curve) and strong ECWS (bottom curve); (b) northern ECWS (>35°N); and (c) those ECWS tracking along the full coast. Data points along the 5-year moving average (black) correspond to the middle year. (Adapted from Hirsch *et al.,* 2001).

The damage from a storm's waves depends to a large extent on whether it makes landfall, when the elevated water levels of its surge combine with the high waves to produce coastal erosion and flooding.

Storms (ECWS)[42]. An ECWS is determined to be "strong" if the maximum wind speed is greater than 23.2 m $s^{-1}$ (45 kt). During the period of 1951-1997, their analysis showed that there were an average of 12 ECWS events occurring each winter (October-April), with a maximum in January, and an average of three strong events (Figure 2.22a). They found a general tendency toward weaker systems over the past few decades, based on a marginally significant (at the p=0.1 level) increase in average storm minimum pressure (not shown). However, their analysis found no statistically significant trends in ECWS frequency for all nor'easters identified in their analysis, specifically for those storms that occurred over the northern portion of the domain (>35°N), or those that traversed full coast (Figure 2.22b, c) during the 46-year period of record used in this study.

[42] According to Hirsch *et al.* (2001), in order to be classified as an ECWS, an area of low pressure is required to (1) have a closed circulation; (2) be located along the east coast of the United States, within the box bounded at 45°N by 65° and 70°W and at 30°N by 75° and 85°W; (3) show general movement from the south-southwest to the north-northeast; and (4) contain winds greater than 10.3 meters per second (20 kt) during at least one 6-hour period.

#### 2.2.3.3 Coastal Waves: Trends of Increasing Heights and Their Extremes

The high wind speeds of hurricanes and extratropical storms generate extremes in the heights and energies of ocean waves. Seasonal and long-term changes in storm intensities and their tracks produce corresponding variations in wave heights and periods along coasts, defining their wave climates (Komar *et al.*, 2008). Waves generated by extratropical storms dominate the oceans at higher latitudes, including the Northeast Pacific along the shores of Canada and the west coast of the United States, and along the Atlantic shores of North America where they occur as destructive Nor'easters. Tropical cyclones dominate the coastal wave climatologies at lower latitudes during the warm season (June-September), including the southeast Atlantic coast of the United States, the Gulf of Mexico, and the Caribbean, while tropical cyclones in the East Pacific generate waves along the western shores of Mexico and Central America. In addition, from mid- to late autumn, tropical cyclones sometimes combine with extratropical storms to generate extreme waves

## BOX 2.2: Extreme Coastal Storm Impacts: "The Perfect Storm" as a True Nor'easter

From a coastal impacts perspective, damage is greatest when large storms are propagating *towards* the coast, which generally results in both a larger storm surge and more long period wave energy (resulting in greater run-up, causing more beach/coastal erosion/damage). Storm intensity (wind speed) is usually greatest in the right-front quadrant of the storm (based on the cyclone's forward movement), so the typical track of east coast winter storms propagating parallel to the coast leaves the most intense part of the storm out to sea. In contrast to storms propagating parallel to the coast, Nor'easters (such as "the Perfect Storm") that propagate from east-to-west in a retrograde track at some point in their lifetime (Figure Box 2.2) can generate much greater surge and greater long period wave energy, and also potentially have the most intense associated winds making landfall along the coast.

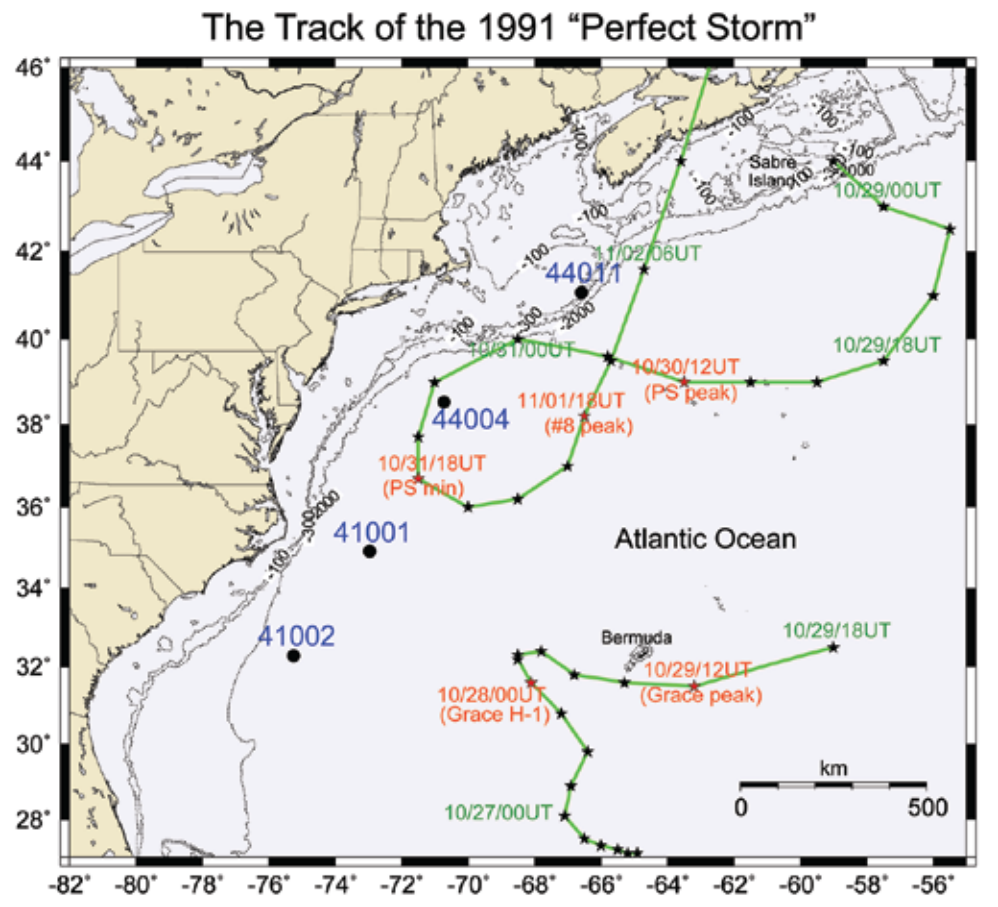


**Figure Box 2.2** Track of the October 1991 "Perfect Storm" (PS) center showing the east-to-west retrograde propagation of a non-typical Nor'easter. The massive ETC was reenergized as it moved southward by absorbing northward propagating remnants of Hurricane Grace, becoming unnamed Hurricane #8 and giving rise to the name "Perfect Storm" for this composite storm. Storm center locations with date/hour time stamps at 6-hour intervals are indicated by stars. Also shown are locations of open ocean NOAA buoys that measured the extreme waves generated by these storms. (Adapted from Bromirski, 2001).

(Bromirski, 2001). The damage from a storm's waves depends to a large extent on whether it makes landfall, when the elevated water levels of its surge combine with the high waves to produce coastal erosion and flooding.

#### *2.2.3.3.1 The Waves of Extratropical Storms and Hurricanes*

The heights of waves generated by a storm depend on its wind speeds, the area over which the winds blow (the storm's fetch), and on the duration of the storm, factors that govern the amount of energy transferred to the waves. The resulting wave energy and related heights have been estimated from: (1) direct measurements

by buoys; (2) visual observations from ships; (3) hindcast analyses[43]; and (4) in recent years from satellite altimetry. The reliability of the data ranges widely for these different sources, depending on the collection methodology and processing techniques. However, multi-decadal records from these sources has made it possible to estimate progressive trends and episodic occurrences of extreme wave heights, and in some cases to establish their underlying causes.

Trends of increasing wave heights have been found along the U.S. Atlantic coast for waves generated by hurricanes.

In the Northern Hemisphere the hurricane winds are strongest on the right-hand side of the storm relative to its track, where the highest winds and rate of storm advance coincide, producing the highest waves within the cyclonic storm. Extreme wave heights are closely associated with the Saffir-Simpson hurricane classification, where the central atmospheric pressures are lower and the associated wind speeds are higher for the more-intense hurricane categories. Correlations have established that on average the measured wave heights and the central atmospheric pressures by Hsu *et al.* (2000) allows the magnitude of the significant wave height[44], $H_S$ to be related to the hurricane category[45]. Estimates of the maximum $H_S$ generated close to the wall of the hurricane's eye in the storm's leading right quadrant, where the wind speeds are greatest, range from about 6 to 7 m for Category 1 storms to 20 m and greater for Category 5. In response to the decreasing wind speeds outward from the eye of the storm, $H_S$ decreases by about 50% at a distance of approximately five times the radius of the eye, typically occurring at about 250 km from the storm's center (Hsu *et al.*, 2000).

This empirically-based model may underpredict the highest waves of Category 4 and 5 storms. Measurements of waves were obtained by six wave gauges deployed at depths of 60 to 90 m in the Gulf of Mexico, when the Category 4 Hurricane Ivan passed directly over the array on 15 September 2004 (Wang *et al.*, 2005). The empirical relationship of Hsu *et al.* (2000) yields a maximum $H_S$ of 15.6 m for Ivan's 935-mb central pressure, seemingly in agreement with the 16 m waves measured by the gauges, but they were positioned about 30 km outward from the zone of strongest winds toward the forward face of Ivan rather than in its right-hand quadrant. Wang *et al.* (2005) therefore concluded it is likely that the maximum significant wave height was greater than 21 m for the Category 4 storm, with the largest individual wave heights having been greater than 40 m, indicating that the Hsu *et al.* (2000) empirical formula somewhat under-predicts the waves generated by high-intensity hurricanes. However, the study by Moon *et al.* (2003) has found that hurricane waves assessed from more complex models that use spatially distributed surface wind measurements compare well with satellite and buoy observations, both in deep water and in shallow water as hurricanes make landfall.

Increasing intensities of hurricanes or of extratropical storms should therefore on average be reflected in upward trends in their generated wave heights. This is evident in the empirical relationship of Hsu *et al.* (2000), which indicates that the significant wave heights should increase from on the order of 5 m to more than 20 m for the range of hurricane categories. Therefore, even a relatively modest increase in average hurricane intensities over the decades might be expected to be detected in measurements of their generated waves.

#### 2.2.3.3.2 Atlantic Coast Waves

Trends of increasing wave heights have been found in wave-buoy measurements along the United States Atlantic coast for waves generated by hurricanes. Komar and Allan

[43] Hindcasts are model estimates of waves using forecast models that are run retrospectively using observed meteorological data.

[44] The "significant wave height" is a commonly used statistical measure for the waves generated by a storm, defined as the average of the highest one-third of the measured wave heights.

[45] Hsu *et al.* (2000) give the empirical formula $H_{smax}=0.2(P_n-P_c)$ where $P_c$ and $P_n \sim 1013$ mbar are respectively the atmospheric pressures at the center and edge of the tropical cyclone, and $H_{smax}$ is the maximum value of the significant wave height.

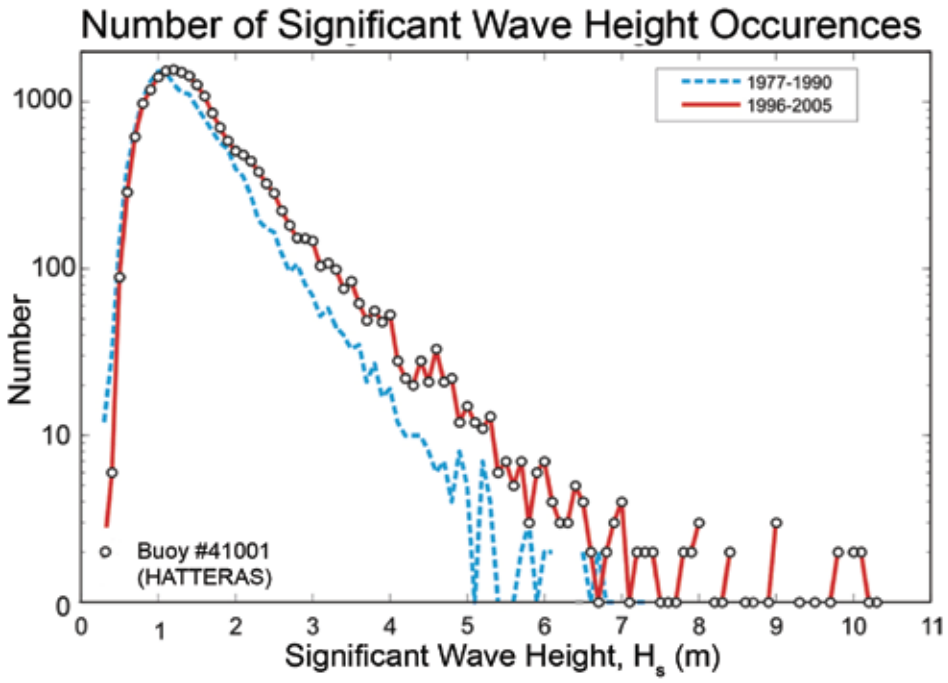


**Figure 2.23** Number of significant wave heights measured by the Cape Hatteras buoy during the July-September season, early in its record 1976-1991 and during the recent decade, 1996-2005 (from Komar and Allan, 2007a,b).

(2007a, 2008) analyzed data from three NOAA buoys located in deep water to the east of Cape May, New Jersey; Cape Hatteras, North Carolina; and offshore from Charleston, South Carolina. These buoys were selected due to their record lengths that began in the mid-1970s, and because the sites represent a range of latitudes where the wave climate is affected by both tropical hurricanes and extratropical storms. Separate analyses were undertaken for the winter season dominated by extratropical storms and the summer season of hurricanes[46], with only the latter having increased. Part of the difficulty in assessing trends in extreme wave heights stems from changes in temporal sampling of the buoy data and the sparse spatial coverage, so it is important to examine the consistency of the resulting buoy analyses with other related measures of wave heights, *e.g.*, hindcasts, changes in storm frequency, tracks, and intensity.

The analyses of the hurricane waves included trends in the annual averages of measured significant wave heights greater than 3 m, as in almost all occurrences they could be identified as having been generated by specific hurricanes (Komar and Allan, 2008). Of the three Atlantic buoys analyzed, the net rate of increase was greatest for that offshore from Charleston (0.59 m/decade, 1.8 m in 30 years). There were several years not included in these analyses due to application of the standard criterion, where a year is excluded, if more than 20% of its potential measurements are missing, the resulting gaps add some uncertainty to the analysis trends. However, the missing years, primarily occurring before 1990, are a mix of very quiet and moderately active hurricane years, thus the finding of an overall increase in significant wave heights is unlikely to have been affected by the missing data. Furthermore, the results are generally consistent with the increase in frequency of hurricane landfalls since the 1970s along the U.S. coasts (Figure 2.17) and the overall increase in the PDI in the Atlantic (Emanuel, 2005a).

The analyses by Komar and Allan (2007a, 2008) also included histograms of all measured significant wave heights for each buoy. Figure 2.23 shows the histograms for Cape Hatteras, one based on data from early in the buoy's record (1977-1990), the second from 1996-2005 (a period of increased hurricane activity in the Atlantic) to document the changes, including the most extreme measured waves[47]. Increases in numbers of occurrences are evident for significant wave heights greater than 2 to 3 m, with regularity in the increases extending up to about 6 m heights, whereas the histograms become irregular for the highest measured waves, the extreme but rare occurrences. Nearly all hurricanes passing through the north Atlantic (not having entered the Gulf of Mexico

The observed increase in the hurricane Power Dissipation Index since the 1970s is consistent with the measured increasing wave heights.

[46] The hurricane waves were analyzed for the months of July through September, expected to be dominated by tropical cyclones, while the waves of extratropical storms were based on the records from November through March; important transitional months such as October were not included, when both types of storms could be expected to be important in wave generation. Also, strict missing data criteria eliminated some years from the analysis that were both quiet and moderately active hurricane years.

[47] Traditionally a wave histogram is graphed as the percentages of occurrences, but in Figure 2.23 the actual numbers of occurrences for the range of wave heights have been plotted, using a log scale that emphasizes the most-extreme heights (Komar and Allan, 2007b)

The intensity of storms outside the tropics has increased in the North Pacific.

or Caribbean) produce measured significant wave heights in the range 3 to 6 m, and this accounts for the decadal trends of increasing annual averages. In contrast, the highest measured significant wave heights are sensitively dependent on the buoy's proximity to the path of the hurricane, being recorded only when the storm passes close to the buoy, with the measured wave heights tending to produce scatter in the data and occasional outliers in the annual averages. This scatter does not lend itself to any statistical conclusions about trends in these most extreme significant wave heights.

Increases in significant wave heights along the United States Atlantic coast therefore depend on changes from year to year in the numbers and intensities of hurricanes, and their tracks, *i.e.*, how closely the storms approached the buoys. Analyses by Komar and Allan (2008) indicate that all of these factors have been important to the observed wave-height increases. The observed increase in the PDI since the 1970s (Figure 2.13) and increases in land-falling hurricane frequency since the 1970s (Figure 2.17) are consistent with the measured increasing wave heights (Figure 2.23).

In contrast to the changes in hurricane waves, analyses of the winter wave heights generated by extratropical storms and recorded since the mid-1970s by the three buoys along the central United States Atlantic shore have shown little change (Komar and Allan, 2007a,b, 2008). This result is in agreement with the hindcast analyses by Wang and Swail (2001) based on the meteorological records of extratropical storms, analyzed with respect to changes in the 90th and 99th percentiles of the significant wave heights, thereby representing the trends for the more extreme wave conditions. A histogram of significant wave heights generated by extratropical storms, measured by the Cape Hatteras buoy during the winter, is similar to the 1996-2005 histogram in Figure 2.23 for the summer hurricane waves, with about the same 10 m extreme measurement (Komar and Allan, 2007b). Therefore, the summer and winter wave climates are now similar despite having different origins, although 30 years ago at the beginning of buoy measurements, the winter waves from extratropical storms were systematically higher than those generated by hurricanes, with the subsequent increase in the latter accounting for their present similarity.

#### *2.2.3.3.3 Pacific Coast Waves*

As reviewed earlier there is evidence that the intensities of extratropical storms have increased in the North Pacific. During strong El Niños, the storms intensify and follow tracks at more southerly latitudes as the Aleutian Low also intensifies and shifts southward (Mo and Livezey, 1986), in contrast to La Niña conditions when tracks are anomalously farther north (Bromirski *et al.*, 2005). These factors have been found to govern the heights of waves measured along the United States West Coast (Seymour *et al.*, 1984; Bromirski *et al.*, 2005; Allan and Komar, 2000). Allan and Komar (2006) analyzed the data from six buoys, from south-central California northward to the coast of Washington, including graphs for the decadal increases in the annual averages of the winter wave heights[48]. The highest rate of increase was found to have occurred on the Washington coast, slightly less offshore from Oregon, with northern to central California being a zone of transition having still lower rates of wave-height increases, until off the coast of south-central California there has not been a statistically significant change. It was further established that some of the "scatter" in the data above and below these linear regressions correlated with the Multivariate ENSO Index, showing that increased wave heights occurred at all latitudes along the U.S. Pacific Coast during major El Niños, but with

[48] "Winter" was taken as the months of October through March, the dominant season of significant storms and of relevance to coastal erosion.

the greatest increases along the shore of southern California where this cycle between El Niños and La Niñas exerts the primary climate control on the storm wave heights and their extremes (Allan and Komar, 2006; Cayan *et al.*, 2008).

More detailed analyses of the extreme wave heights measured off the Washington coast have been undertaken (important with respect to erosion), with example trends graphed in Figure 2.24 and a complete listing of the regression results in Table 2.1 (Allan and Komar, 2006). The annual averages of the winter wave heights and the averages of the five largest significant wave heights measured each winter have been increasing, the latter showing a higher rate of increase (0.95 m/decade, a 2.85 m increase in the significant wave heights in 30 years). The series of analyses demonstrate that the higher waves are increasing faster, at a rate of about 1 m/decade for the single highest measured significant wave height each year. This pattern of increase is reflected in progressive shifts in the histograms of measured significant wave heights, like that seen in Figure 2.23 for the East Coast hurricane-generated waves, with the orderly progression in Table 2.1 reflecting the increasing skewness of the histograms for the ranges of most extreme measured waves (Komar *et al.*, 2008).

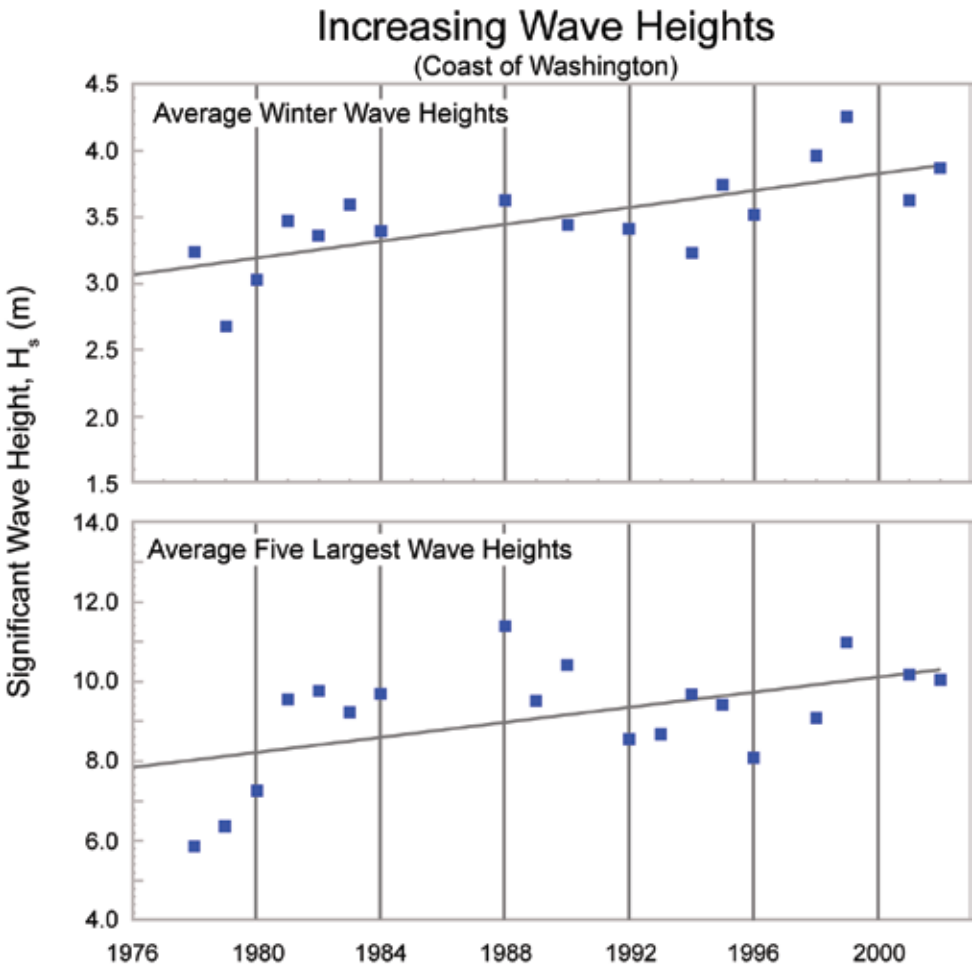


**Figure 2.24** The trends of increasing wave heights measured by NOAA's National Data Buoy Center (NDBC) buoy #46005 off the coast of Washington (after Allan and Komar, 2006).

While the linear trends for averages of the largest five storm-wave occurrences each year are statistically significant at the 0.05 significance level (Figure 2.24), the linear trends for the more extreme waves are not statistically significant (Table 2.1). However, in analyses using other statistical models, changes in the most extreme measured wave heights are also statistically significant (Komar *et al.*, 2008).

The identification of varying wave heights in the North Pacific affected by climate variations and changes is limited by the relatively short record length from the buoys, extending back only to the 1970s. Visual observations from ships in transit provide longer time series of wave height estimates, but of questionable quality. Gulev and Grigorieva (2004) examined this source of wave data for the North Pacific, finding that there has been a general increase in the significant wave heights beginning in about 1960, in agreement with that found by the wave buoy measurements (Figure 2.24). The wave hindcasts by Wang and Swail (2001) also show a general increase in the 90th and 99th percentile wave heights throughout the central to eastern North Pacific.

There has been a northward shift in heavy snowstorm occurrence for the U.S. and Canada.

### 2.2.3.4 Winter Storms

#### *2.2.3.4.1 Snowstorms*

The amount of snow that causes serious impacts varies depending on a given location's usual snow conditions. A snowstorm is defined here as an event in which more than 15 cm of snow

Snow cover extent for North America abruptly decreased in the mid-1980s and generally has remained low since then.

falls in 24 hours or less at some location in the United States. This is an amount sufficient to cause societally-important impacts in most locations. During the 1901-2001 period, 2,257 snowstorms occurred (Changnon *et al.*, 2006). Temporal assessment of the snowstorm incidences during 1901-2000 revealed major regional differences. Comparison of the storm occurrences in 1901-1950 against those in 1951-2000 revealed that much of the eastern United States had more storms in the early half of the 20th century, whereas in the West and New England, the last half of the century had more storms. Nationally, 53% of the weather stations had their peaks in 1901-1950 and 47% peaked in 1951-2000.

The South and lower Midwest had distinct statistically significant downward trends in snowstorm frequency from 1901 to 2000. In direct contrast, the Northeast and upper Midwest had statistically significant upward linear trends, although with considerable decade-to-decade variability. These contrasting regional trends suggest a net northward shift in snowstorm occurrence over the 20th century. Nationally, the regionally varying up and down trends resulted in a national storm trend that was not statistically significant for 1901-2000. Research has shown that cyclonic activity was low during 1931-1950, a period of few snowstorms in the United States.

In the United States, 39 of 231 stations with long-term records had their lowest frequencies of storms during 1931-1940, whereas 29 others had their peak of incidences then. The second ranked decade with numerous stations having low snowstorm frequencies was 1981-1990. Very few low storm occurrences were found during 1911-1920 and in the 1961-1980 period, times when storms were quite frequent. The 1911-1920 decade had the greatest number of high station values with 38 stations. The fewest peak values occurred in the next decade, 1921-1930. Comparison of the decades of high and low frequencies of snowstorms reveals, as expected, an inverse relationship. That is, when many high storm values occurred, there are few low storm frequencies.

Changes in heavy snowfall frequency have been observed in Canada (Zhang *et al.*, 2001). In southern Canada, the number of heavy snowfall events increased from the beginning of the 20th century until the late 1950s to the 1970s, then decreased to the present. By contrast, heavy snowfall events in northern Canada have been increasing with marked decade-to-decade variation.

The analyses of United States and Canadian heavy snowfall trends both suggest a northward shift in the tracks of heavy snowfall storms, but it is unclear why southern Canadian data reveal a decrease in heavy snowstorms since 1970. Specifically, the upward trend in heavy snowstorms in the United States over the past several decades is absent in adjacent southern Canada. To date, no analyses have been completed to better understand these differences.

In the United States, the decades with high snowstorm frequencies were characterized by cold winters and springs, especially in the West. The three highest decades for snowstorms (1911-1920, 1961-1970, and 1971-1980) were ranked 1st, 4th, and 3rd coldest, respectively, while the two lowest decades (1921-1930 and 1931-1940) were ranked as 3rd and 4th warmest. One exception to this general relationship is the warmest decade (1991-2000), which experienced a moderately high number of snowstorms across the United States.

Very snowy seasons (those with seasonal snowfall totals exceeding the 90th percentile threshold) were infrequent in the 1920s and 1930s and have also been rare since the mid-1980s (Kunkel *et al.*, 2007b). There is a high correlation with average winter temperature. Warm winters tend to have few stations with high snowfall totals, and most of the snowy seasons have also been cold.

Some of the snowiest regions in North America are the southern and eastern shores of the Great Lakes, where cold northwesterly winds flowing over the warmer lakes pick up moisture and deposit it on the shoreline areas. There is evidence of upward trends in snowfall since 1951 in these regions even while locations away from the snowy shoreline areas have not experienced increases (Burnett *et al.*, 2003). An analysis of historical heavy lake-effect snowstorms identified several weather conditions to be closely related to heavy lake-effect snowstorm occurrence including moderately high surface wind speed, wind direction promoting a long fetch over the lakes, surface air temperature in the range of -10 to 0°C, lake surface to air temperature difference of at least 7°C, and an unstable lower troposphere (Kunkel *et al.*, 2002). It is also necessary that the lakes be mostly ice-free.

Snow cover extent for North America based on satellite data (Robinson *et al.*, 1993) abruptly decreased in the mid-1980s and generally has remained low since then (http://climate.rutgers.edu/snowcover/chart_anom.php?ui_set=0&ui_region=nam&ui_month=6).

#### *2.2.3.4.2 Ice Storms*

Freezing rain is a phenomenon where even light amounts can have substantial impacts. All days with freezing rain (ZR) were determined during the 1948-2000 period based on data from 988 stations across the United States (Changnon and Karl, 2003). The national frequency of freezing rain days (FZRA) exhibited a downward trend, being higher during 1948-1964 than in any subsequent period.

The temporal distributions of FZRA for three climate regions (Northeast, Southeast, and South) reveal substantial variability. They all were high in 1977-1980, low in 1985-1988, and

lowest in 1973-1976. The 52-year linear trends for all three regions were downward over time. The time distributions for the Central, West North Central, and East North Central regions are alike, all showing that high values occurred early (1949-1956). All climate regions had their lowest FZRA during 1965-1976. The East North Central, Central, Northwest, and Northeast regions, which embrace the northern half of the conterminous United States, all had statistically significant downward linear trends. This is in contrast to trends in snowstorm incidences.

The national frequency of freezing rain days has exhibited a downward trend, being higher during 1948-1964 than in any subsequent period.

Both snowstorms and ice storms are often accompanied or followed by extreme cold because a strong ETC (which is the meteorological cause of the snow and ice) is one of the meteorological components of the flow of extreme cold air from the Arctic. This compounds the impacts of such events in a variety of ways, including increasing the risks to human health and adversely affecting the working environment for snow removal and repair activities. While there have been no systematic studies of trends in such compound events, observed variations in these events appear to be correlated. For example, the late 1970s were characterized both by a high frequency of extreme cold (Kunkel *et al.*, 1999a) and a high frequency of high snowfall years (Kunkel *et al.*, 2007b).

### 2.2.3.5 Convective Storms

Thunderstorms in the United States are defined to be severe by the National Weather Service (NWS) if they produce hail of at least 1.9 cm

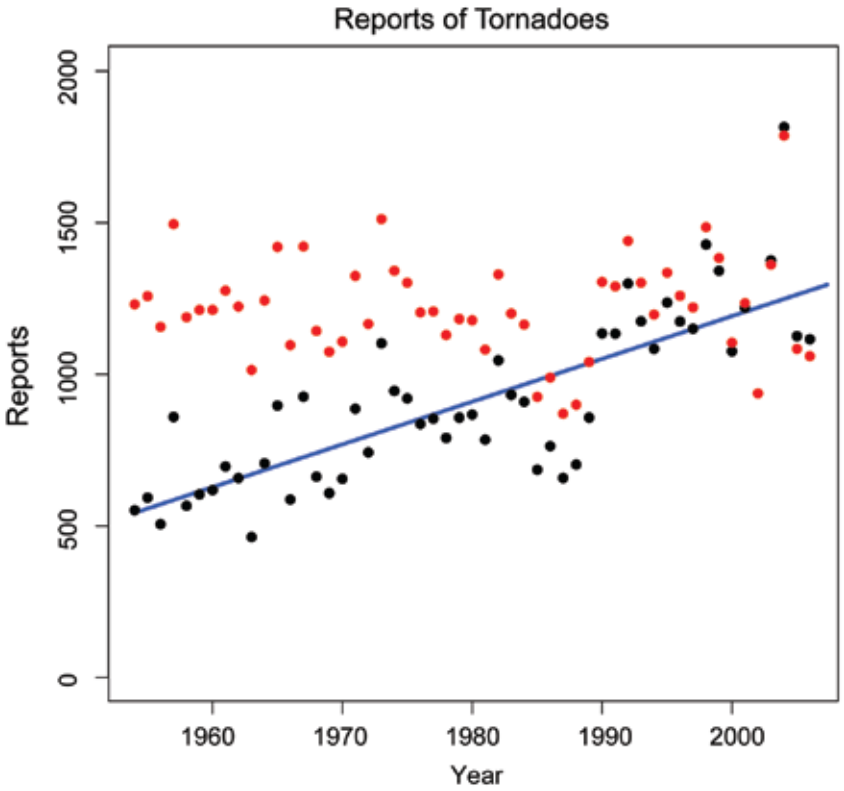


**Figure 2.25** Tornado reports in official database in the United States from 1954-2004. Black circles are raw reports, solid line (linear regression) is the trend for raw reports, red circles are reports adjusted to 2002 reporting system. The adjusted data show little or no trend in reported tornadoes. The trend in raw reports reflects an increasing density of population in tornado-prone areas, and therefore more opportunity for sightings, rather than a real increase in the occurrences of tornadoes.

(3/4 inch) in diameter, wind gusts of at least 25.5 m per second (50 kt), or a tornado. Currently, reports come from a variety of sources to the local NWS forecast offices that produce a final listing of events for their area. Over the years, procedures and efforts to produce that listing have changed. Official data collection in near- real time began in 1953 for tornadoes and 1955 for hail and wind. Prior to 1973, tornado reports were verified by state climatologists (Changnon, 1982). In addition, efforts to improve verification of severe thunderstorm and tornado warnings, the introduction of Doppler radars, changes in population, and increases in public awareness have led to increases in reports over the years. Changes in reporting practices have also led to inconsistencies in many aspects of the records (*e.g.*, Brooks, 2004). Changnon and Changnon (2000) identified regional changes in hail frequency from reports made at official surface observing sites. With the change to automated surface observing sites in the 1990s, the number of hail reports at those locations dropped dramatically because of the loss of human observers at the sites. As a result, comparisons to the Changnon and Changnon work cannot be continued, although Changnon *et al.* (2001) have attempted to use insurance loss records as a proxy for hail occurrence.

The raw reports of annual tornado occurrences show an approximate doubling from 1954-2003 (Brooks and Dotzek, 2008), a reflection of the changes in observing and reporting. When detrended to remove this artificial trend, the data show large interannual variability, but a persistent minimum in the late 1980s (Figure 2.25). There were changes in assigning intensity estimates in the mid-1970s that resulted in tornadoes prior to 1975 being rated more strongly than those in the later part of the record (Verbout *et al.*, 2006). More recently, there have been no tornadoes rated F5, the highest rating, since 3 May 1999, the longest gap on record. Coupled with a large decrease in the number of F4 tornadoes (McCarthy *et al.*, 2006), it has been suggested that the strongest tornadoes are now being rated lower than practice prior to 2000.

A data set of F2 and stronger tornadoes extending back before the official record (Grazulis, 1993) provides an opportunity to examine longer trends. This examination[49] of the record

[49] This analysis used the technique described in Brooks *et al.* (2003a) to estimate the spatial distribution over

from 1921-1995 indicates that the variability between periods was large, without significant long-term trends (Concannon *et al.*, 2000).

The fraction of strong tornadoes (F2 and greater) that have been rated as violent (F4 and greater) has been relatively consistent in the U.S. from the 1950s through the 1990s[50] (Brooks and Doswell, 2001)[51]. There were no significant changes in the high-intensity end of these distributions from the 1950s through the 1990s, although the distribution from 2000 and later may differ.

Reports of severe thunderstorms without tornadoes have increased even more rapidly than tornado reports (Doswell *et al.*, 2005, 2006). Over the period 1955-2004, this increase was approximately exponential, resulting in an almost 20-fold increase over the period. The increase is mostly in marginally severe thunderstorm reports (Brooks, 2007). An overall increase is seen, but the distribution by intensity is similar in the 1970s and post-2000 eras for the strongest 10% of reports of hail and wind. Thus, there is no evidence for a change in the severity of events, and the large changes in the overall number of reports make it impossible to detect if meteorological changes have occurred.

Environmental conditions that are most likely associated with severe and tornado-producing thunderstorms have been derived from reanalysis data (Brooks *et al.*, 2003b), and counts of the frequency of favorable environments for significant severe thunderstorms[52] have been determined for the area east of the Rocky Mountains in the U.S. for the period 1958-1999 (Brooks and Dotzek, 2008). The count of favorable environments decreased from the late 1950s into the early 1970s and increased after that through the 1990s, so that the frequency was approximately the same at both ends of the analyzed period. Given the high values seen at the beginning of the reanalysis era, it is likely that the record is long enough to sample natural variability, so that it is possible that even though the 1973-1999 increase is statistically significant, it does not represent a departure from natural variability. The time series of the count of reports of very large hail (7 cm diameter and larger) shows an inflection at about the same time as the inflection in the counts of favorable environments. A comparison of the rate of increase of the two series suggested that the change in environments could account for approximately 7% of the change in reports from the mid-1970s through 1999, with the rest coming from non-meteorological sources. Changes in tornado reports do not correspond to the changes in overall favorable severe thunderstorm environment, in part because the discrimination of environments favorable for tornadoes in the reanalysis data is not as good as the discrimination of severe thunderstorm environments (Brooks *et al.*, 2003a).

There is no evidence for a change in the severity of tornadoes and severe thunderstorms, and the large changes in the overall number of reports make it impossible to detect if meteorological changes have occurred.

different periods.

[50] Note that consistent overrating will not change this ratio.

[51] Feuerstein *et al.* (2005) showed that the distribution in the U.S. and other countries could be fit to Weibull distributions with the parameters in the distribution converging as time goes along, which they associated with more complete reporting of events.

[52] Hail of at least 5 cm diameter, wind gusts of at least 33 m $s^{-1}$, and/or a tornado of F2 or greater intensity.

## 2.3 KEY UNCERTAINTIES RELATED TO MEASURING SPECIFIC VARIATIONS AND CHANGE

For trends beginning in the late 1800s the changing spatial coverage of the data set is a concern.

In this section, we review the statistical methods that have been used to assess uncertainties in studies of changing extremes. The focus of the discussion is on precipitation events, though similar methods have also been used for temperature.

### 2.3.1 Methods Based on Counting Exceedances Over a High Threshold

Most existing methods follow some variant of the following procedure, given by Kunkel *et al.* (1999b). First, daily data are collected, corrected for biases such as winter undercatchment. Only stations with nearly complete data are used (typically, "nearly complete" means no more than 5% missing values). Different event durations (for example, 1-day or 7-day) and different return periods (such as 1-year or 5-year) are considered. For each station, a threshold is determined according to the desired return value. For example, with 100 years of data and a 5-year return value, the threshold is the 20th largest event. The number of exceedances of the threshold is computed for each year, and then averaged either regionally or nationally. The averaging is a weighted average in which, first, simple averaging is used over climate divisions (typically there are about seven climate divisions in each state), and then, an area-weighted average is computed over climate divisions, either for one of the nine U.S. climate regions or the whole contiguous United States. This averaging method ensures that parts of the country with relatively sparse data coverage are adequately represented in the final average. Sometimes (*e.g.,* Groisman *et al.*, 2005; Kunkel *et al.*, 2007a) the climate divisions are replaced by 1° by 1° grid cells. Two additional refinements used by Groisman *et al.* (2005) are: (i) to replace the raw exceedance counts for each year by anomalies from a 30-year reference period, computed separately for each station and (ii) to assess the standard error of the regional average using spatial statistics techniques. This calculation is based on an exponentially decreasing spatial covariance function with a range of the order 100-500 km and a nugget:sill ratio (the proportion of the variability that is not spatially correlated) between 0 and 85%, depending on the region, season, and threshold.

Once these spatially averaged annual exceedance counts or anomalies are computed, the next step is to compute trends. In most studies, the emphasis is on linear trends computed either by least squares regression or by the Kendall slope method, in which the trend is estimated as the median of all possible slopes computed from pairs of data points. The standard errors of the trends should theoretically be corrected for autocorrelation, but in the case of extreme events, the autocorrelation is usually negligible (Groisman *et al.*, 2004).

One of the concerns about this methodology is the effect of changing spatial coverage of the data set, especially for comparisons that go back to the late years of the 19th century. Kunkel *et al.* (2007a) generated simulations of the 1895-2004 data record by first randomly sampling complete years of data from a modern network of 6,351 stations for 1971-2000, projecting to a random subnetwork equivalent in size and spatial extent to the historical

data network, then using repeat simulations to calculate means and 95% confidence intervals for five 22-year periods. The confidence intervals were then superimposed on the actual 22-year means calculated from the observational data record. The results for 1-year, 5-year, and 20-year return values show clearly that the most recent period (1983-2004) has the highest return values of the five periods, but they also show the second highest return values in 1895-1916 with a sharp drop thereafter, implying a role that is still not fully explained due to natural variability.

Some issues that might justify further research include the following:

1. Further exploration of why extreme precipitation apparently decreases after the 1895-1916 period before the recent (post-1983) rise when they exceeded that level. For example, if one breaks the data down into finer resolution spatially, does one still see the same effect?
2. What about the effect of large-scale circulation effects such as ENSO events, AMO, PDO, *etc.*? These could potentially be included as covariates in a time series regression analysis, thus allowing one to "correct" for circulation effects in measuring the trend.
3. The spatial analyses of Groisman *et al.* (2005) allow for spatial correlation in assessing the significance of trends, but they don't do the logical next step, which is to use the covariance function to construct optimal interpolations (also known as "kriging") and thereby produce more detailed spatial maps. This is something that might be explored in the future.

### 2.3.2 The GEV Approach

An alternative approach to extreme value assessment is through the Generalized Extreme Value (GEV) distribution[53] and its variants. The GEV combines three "types" of extreme value distributions that in earlier treatments were often regarded as separate families (*e.g.*, Gumbel, 1958). The distribution is most frequently applied to the annual maxima of a meteorological or hydrological variable, though it can also be applied to maxima over other time periods (*e.g.*, one month or one season). With minor changes in notation, the distributions are also applicable to minima rather than maxima. The parameters may be estimated by maximum likelihood, though there are also a number of more specialized techniques such as L-moments estimation. The methods have been applied in climate researchers by a number of authors including Kharin and Zwiers (2000), Wehner (2004, 2005), Kharin *et al.* (2007).

There is more to be learned about the effects of large scale circulation patterns, such as the El Niño Southern Oscillation, on extreme events

The potential advantage of GEV methods over those based on counting threshold exceedances is that by fitting a probability distribution to the extremes, one obtains more information that is less sensitive to the choice of threshold, and can also derive other quantities such as the $T$-year return value $X_T$, calculated by solving the equation $F(X_T)=1-1/T$. Trends in the $T$-year return value (for typical values of $T$, *e.g.*, 1, 10, 25, or 100 years) would be particularly valuable as indicators of changing extremes in the climate.

[53] The basic GEV distribution is given by the formula (see, *e.g.*, Zwiers and Kharin, 1998):
$F(x) = \exp\{-[1-k(x-\xi)/\alpha]^{1/k}\}$ in which $\xi$ plays the role of a centering or location constant, $\alpha$ determines the scale, and $k$ is a key parameter that determines the shape of the distribution. (Other authors have used different notations, especially for the shape parameter.) The range of the distribution is:
$x<\xi+\alpha/k$ when $k<0$, $x>\xi+\alpha/k$ when $k<0$, $-\infty<x<\infty$ when $k=0$, in which case the formula reduces to $F(x) = \exp\{-\exp[-(x-\xi)/\alpha]\}$ and is known as the Gumbel distribution.

Direct application of GEV methods is often inefficient because they only use very sparse summaries of the data (typically one value per year), and need reasonably long time series before they are applicable at all. Alternative methods are based on exceedances over thresholds, not just counting exceedances but also fitting a distribution to the excess over the threshold. The most common choice of distribution of excess is the Generalized Pareto distribution or GPD, which is closely related to the GEV (Pickands, 1975; Davison and Smith, 1990). Some recent overviews of extreme value distributions, threshold methods, and a variety of extensions are by Coles (2001) and Smith (2003).

Much of the recent research (*e.g.*, Wehner, 2005; Kharin *et al.*, 2007) has used model output data, using the GEV to estimate, for example, a 20-year return value at each grid cell, then plotting spatial maps of the resulting estimates. Corresponding maps based on observational data must take into account the irregular spatial distribution of weather stations, but this is also possible using spatial statistics (or kriging) methodology. For example, Cooley *et al.* (2007) have applied a hierarchical modeling approach to precipitation data from the Front Range of Colorado, fitting a GPD to threshold exceedances at each station and combining results from different stations through a spatial model to compute a map of 25-year return values. Smith *et al.* (2008) applied similar methodology to data from the whole contiguous United States, producing spatial maps of return values and also calculating changes in return values over the 1970-1999 period.

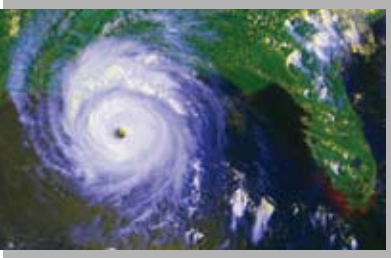

# Weather and Climate Extremes in a Changing Climate

## Regions of Focus: North America, Hawaii, Caribbean, and U.S. Pacific Islands

Synthesis and Assessment Product 3.3
Report by the U.S. Climate Change Science Program
and the Subcommittee on Global Change Research

EDITED BY:
Thomas R. Karl, Gerald A. Meehl, Christopher D. Miller, Susan J. Hassol,
Anne M. Waple, and William L. Murray